OFFICE OF NAVAL RESEARCH

GRANT or CONTRACT: N00014-91-J-1919

R&T Code 4133036
Robert Nowak

Technical Report No. 15

Preparation of Au Single Crystals for Study of the ECALE Deposition of CdTe

Laura B. Goetting, Baoming M. Huang, Tedd E. Lister and John L. Stickney

In Press

for

Electrochemica Acta

Department of Chemistry
University of Georgia
Athens, GA 30602-2556

6/24/94

REPORT DOCUMENTATION PAGE

Form Approved
OMB No 0704-0188

1. AGENCY USE ONLY (Leave blank)	2. REPORT DATE	3. REPORT TYPE AND DATES COVERED
	6/25/94	Technical - 1, June

4. TITLE AND SUBTITLE
Preparation of Au Single Crystals for Studies of the ECALE Deposition of CdTe

5. FUNDING NUMBERS
G-N00014-19-J-1919

6. AUTHOR(S)
Laura B. Goetting, Baoming M. Huang, Tedd E. Lister and John L. Stickney

7. PERFORMING ORGANIZATION NAME(S) AND ADDRESS(ES)
John L. Stickney
Department of Chemistry
University of Georgia
Athens, GA 30602-2556

8. PERFORMING ORGANIZATION REPORT NUMBER
Technical Report #15

9. SPONSORING / MONITORING AGENCY NAME(S) AND ADDRESS(ES)
Office of Naval Research
Chemistry Division
Arlington, CA 22217-5000

10. SPONSORING / MONITORING AGENCY REPORT NUMBER

11. SUPPLEMENTARY NOTES

12a. DISTRIBUTION / AVAILABILITY STATEMENT
Approved for public release and sale;
its distribution is unlimited

12b. DISTRIBUTION CODE

13. ABSTRACT *(Maximum 200 words)*

A sequence of questions concerning the preparation of atomically flat Au surfaces is addressed. In addition, the formation of a 1/2 monolayer Te adlayer of a Au(100) is discussed. The 1/2 coverage of Au(100)-Te surface is desired as a first step in the electrodeposition of CdTe by the ECALE methodology. The use of oxidation/reduction cycles (ORCs) to clean the Au(100) surface is shown to be counter productive, if atomically flat planes are also desired. Roughening results from the ORCs as the surface reconstructs at low potentials, then unreconstructs at high potentials. The reconstructed surface contains excess surface atoms, such that upon lifting of the reconstruction, monoatomically high Au islands are formed on the surface. It is also shown that treatment in a mM I^- solution results in the formation of ordered iodine adlattices on each of the low index planes. In addition, electrochemical annealing is facilitated, resulting in removal of previously formed Au islands, and formation of large, atomically flat terraces. Te can be deposited directly on these I coated surfaces, displacing the I and forming thin films of bulk Te. The excess, bulk, Te can then be removed either reductively or oxidatively, to form ordered atomic layers of Te with coverages near 1/2.

14. SUBJECT TERMS
Au, single crystals, Iodine, CdTe, ECALE, reconstructions

15. NUMBER OF PAGES
47

16. PRICE CODE

17. SECURITY CLASSIFICATION OF REPORT	18. SECURITY CLASSIFICATION OF THIS PAGE	19. SECURITY CLASSIFICATION OF ABSTRACT	20. LIMITATION OF ABSTRACT
Unclassified	Unclassified	Unclassified	UL

PREPARATION OF Au SINGLE CRYSTALS FOR STUDIES OF THE ECALE DEPOSITION OF CdTe

Laura B. Goetting, Baoming M. Huang, Tedd E. Lister and John L. Stickney*

Department of Chemistry, University of Georgia, Athens, Georgia 30602

* To whom correspondence should be addressed.

ABSTRACT

A sequence of questions concerning the preparation of atomically flat Au surfaces is addressed. In addition, the formation of a 1/2 monolayer Te adlayer on a Au(100) is discussed. The 1/2 coverage Au(100)-Te surface is desired as a first step in the electrodeposition of CdTe by the ECALE methodology. The use of oxidation/reduction cycles (ORCs) to clean the Au(100) surface is shown to be counter productive, if atomically flat planes are also desired. Roughening results from the ORCs as the surface reconstructs at low potentials, then unreconstructs at high potentials. The reconstructed surface contains excess surface atoms, such that upon lifting of the reconstruction, monoatomically high Au islands are formed on the surface. It is also shown that treatment in a mM I^- solution results in the formation of ordered iodine adlattices on each of the low index planes. In addition, electrochemical annealing is facilitated, resulting in removal of previously formed Au islands, and formation of large, atomically flat terraces. Te can be deposited directly on these I coated surfaces, displacing the I and forming thin films of bulk Te. The excess, bulk, Te can then be removed either reductively or oxidatively, to form ordered atomic layers of Te with coverages near 1/2.

INTRODUCTION

A new methodology for the electrochemical formation of thin films of compounds, electrochemical atomic layer epitaxy (ECALE), is presently being studied and developed in our laboratory [1, 2]. ECALE is the electrochemical analogue of atomic layer epitaxy (ALE) [3-5], where ALE is a methodology involving the alternated deposition of atomic layers of the individual elements forming a compound. Surface confined reactions are used to limit the deposition of an element to one atomic layer at a time. Theoretically, epitaxial deposits will result if the cycle involves formation of complete atomic layers for each element, avoiding three dimensional nucleation. In addition, ALE provides sensitive control over the deposit thickness, as the number of cycles is a direct measure.

The ALE methodology has been applied, for the most part, to chemical vapor deposition (CVD) and molecular beam epitaxy (MBE) systems, where reactivity is generally controlled by the substrate temperature. In ECALE, reactivity is limited to an atomic layer of a given element by using underpotential deposition (UPD) [6-8]. The basic ECALE deposition cycle involves formation of an atomic layer of one element at its underpotential, from a solution of its precursor, followed by exchange of the solution for one containing the precursor of the second element. An atomic layer of the second element is then deposited at its underpotential, completing deposition of one monolayer of a binary compound. The cycle is then repeated, with each repetition resulting in the formation of another monolayer of the compound.

Breaking up compound electrodeposition into a cycle composed of a set of discrete steps should result in significantly increased control. In addition, breaking up the process provides an opportunity to study the individual steps, in a relatively static mode. An atomic level picture of the surface chemistry central to the various steps in the cycle is presently being developed. Key

questions to be answered involve the importance of substrate structure and composition, as well as the determination of the coverages and structures that result after each step in the ECALE cycle, and the variance of each with potential and solution composition. Previous studies have included investigations of the structures formed by the deposition of atomic layers of Te on the low index planes of Au [9, 10]. Those studies revealed the Te unit cells and bases formed by Te UPD. Subsequent studies have, however, indicated the presence of a large number of islands on the surfaces used in those studies, raising the question: were the islands initially present on the substrate, or were they a result of the deposition process? Further, how can they be avoided? The work described here was performed to address these questions.

EXPERIMENTAL

Several Au single crystals were used in these studies, including: a 1 cm diameter Au(100) slice, 0.2 cm thick; a six sided Au(100); and a Au tri-crystal. The six sided Au(100) crystal was constructed such that six faces were oriented, cut, and polished to display the same (100) atomic geometry on all surfaces. This crystal was especially valuable in coulometric studies and studies of the voltammetry specific to the (100) plane, as the entire crystal could be immersed. The tri-crystal was constructed such that three faces were oriented, cut and polished, each to a different low-index plane: (100), (110) and (111). In addition, each face was parallel to a central axis. In that way, the crystal could be rotated about the axis and each face studied in turn. The tri-crystal was used to simultaneously survey the reactivity of the three low-index planes under equivalent conditions.

All crystals were first oriented using Laue back reflection X-ray diffraction, using a two axis goniometer from South Bay Technology, San Clemente, CA. The goniometer was designed

to fit in the bottom of a hand held polishing jig, also from South Bay Technology. Once the sample had been oriented using a Philips X-ray source, the goniometer was easily transferred to the polishing jig without loss of the orientation information. It was then a simple matter to polish the crystal surface parallel to the desired plane.

Polishing was accomplished using successively finer grades of aluminum oxide polishing films, finishing with 0.3μm grit film. After removal of the potting wax, the crystals were electropolished in a cyanide bath for 5 minutes at 1.5 A/cm^2 [11]. Inspection using an optical microscope, 1000X, revealed a very flat surface with no evidence of scratches from the polishing grits.

After each experiment, the crystal was cleaned in concentrated HNO_3, flamed in a gas oxygen torch, and quenched in DI water.

Studies of the surface structure of the Au crystals were carried out using a combined UHV-EC surface analysis instrument [12]. The instrument is equipped with optics for low-energy electron diffraction (LEED), Auger electron spectroscopy (AES), and X-ray photoelectron spectroscopy (XPS). The surface analysis chamber was also equipped with an isolatable antechamber where electrochemical experiments were performed without exposure of the sample to air. Scanning tunneling microscopic (STM) investigations were performed in air using a Nanoscope III (Digital Instruments, Santa Barbara CA).

Solutions were prepared with high purity reagents and water from a Nanopure DI water system, fed from the house distilled water system. The solutions used in the studies were as follows: 5 mM KI (Baker Analyzed) + 20 mM H_2SO_4 (Baker Analyzed), pH 1.5; 0.2 mM TeO_2

(Johnson Matthey); 20 mM H_2SO_4, pH 1.5; 0.5 M Na_2SO_4 (Baker Analyzed); 10 mM $Na_2B_4O_7$ (Baker Analyzed), pH 9.

A Ag/AgCl (1M NaCl) reference electrode was used in the studies described below. The potentiostats were built in-house and were of a conventional op-amp design.

RESULTS AND DISCUSSIONS:

Substrates used in initial studies of the formation of atomic layers of Te on Au single crystals [9, 10] were prepared as described above. In addition, once the electrodes were immersed, several oxidation/reduction cycles (ORC) were performed in 1 M H_2SO_4, between -0.5 V and 1.3 V, as a final cleaning step. Small scale STM micrographs taken of these surfaces after deposition of Te showed atomic scale structure [10] consistent with previously observed unit cells determined using LEED [9]. Subsequent studies on more accurately oriented substrates, with larger terraces, revealed a significant number of monoatomically high Au islands. These islands were evident both before and after Te deposition (Figure 1). Recently published accounts by other workers have indicated that islands on Au(100) can result from the ORCs. It has been shown that the square Au(100) surface undergoes a reconstruction in solution at negative potentials, below -0.25 V in mM H_2SO_4, to a columnar structure where the surface atoms have adopted a hexagonal arrangement [13-17]. The reconstructed Au(100) surface (Hex [18]) contains about 20-24% more surface atoms then the corresponding unreconstructed surface [19, 20] (Figure 2). Conversely, the surface reconstruction is removed at positive potentials, above 0.6 V, leaving the extra surface atoms available to form islands [18, 21] (Figure 3). The sizes of the islands are a function of several variables, including time. The Au atoms have

sufficient mobility that, on a time scale of an hour or more, the smaller islands coalesce into larger islands or merge with step edges [22-25].

By alternating the electrode potential between -0.5 V and 1.3 V, such as in an ORC, the surface is repeatedly reconstructed and then unreconstructed, each cycle forming still more islands. ORCs should clearly not be a part of a surface cleaning procedure if islands are to be avoided. Even if ORCs are avoided, there is still the problem that some degree of reconstruction accompanies the flame treatment, depending on the subsequent quenching procedure used [21, 26, 27]. Immersion of the partially reconstructed surface at a positive potential removes the reconstruction, again resulting in the formation of islands.

One solution to the island formation is to "electrochemically anneal" the surface [18, 28]. There is evidence that adsorbed electrolytes, such as halides, can remove surface reconstructions and islands. This observation may be the result of two separate effects. The reconstructions may be lifted because the halide adsorption process significantly changes the energetics of the Au surface, making the reconstruction less favorable, the islands may be removed because the halide increases the mobility of the Au surface atoms [29], allowing them to combine with step edges. Alternatively, the halide ions may be facilitating a leveling etch of the surface [30].

Previous work investigating the adsorption of iodide on Au [31] prompted the present investigation of the effect of a mM iodide solution on Au surface leveling. Well-ordered I atom adlattices were observed on each of the low index planes of Au exposed to the iodide. An initial study of the structures formed by iodide on Au(111) was performed using LEED and Auger spectroscopy [31]. A series of well-ordered adlattices were observed, including: a (4X4)-CsI structure, a $(\sqrt{3}\ X\sqrt{3}\ )R30°$-I, and a $(5X\sqrt{3}\ )$ -I. The structures were formed in the order stated, as the potential was increased, and each was formed with a successively higher I coverage (θ =

0.25, 0.33, and 0.4 respectively). Subsequent studies using STM [32-34] have led to similar conclusions, especially concerning the formation of a structure with a ($5X\sqrt{3}$) unit-cell. Additionally, it has been shown in an elegant in-situ X-ray scattering study that the size of the iodine adlattice unit cell in solution is a smooth function of potential: the iodine adlattice constants decreased as the potential increased [35].

Well-ordered I adlattices have also been formed on Au(110) and Au(100). Studies of those faces have been performed using STM [28, 36-38], and, in the present study, using LEED, AES and STM. Figure 4 is a LEED pattern obtained from a Au(110) surface after emersion from a 1 mM I^- solution at -0.16 V. The pattern is indicative of a (3X2) unit cell. Comparisons of the iodine Auger signal with those observed for structures on Au(111), indicate a coverage greater than 1/2. The observed unit cell and coverage are consistent with STM micrographs such as that shown in Figure 5. A proposed structure is shown in Figure 6, which is equivalent to that previously proposed for Cl adsorbed on Cu(110) [39]. I atoms have been drawn at their van der Waals diameter, 0.43 nm [40]. Similar micrographs have been observed, and structures proposed, in other studies of iodide adsorption [36, 37].

The structures observed on the Au(100) surface are not as straightforward as the Au(110)(3X2)-I. The LEED pattern observed for the crystal emersed from an I^- solution at -0.16V is shown in Figure 7. The unit cell of the pattern is not immediately obvious. Similar LEED patterns have been observed in at least two other studies, one concerning the adsorption of I_2 on Au(100) in UHV [41], and the other concerning the adsorption of HI on Pt(100) [42]. In both cases, the I atom coverage was near 0.43. At coverages closer to 0.5, ($\sqrt{2}$ X$2\sqrt{2}$)R45° -I structures were obtained in both previous studies [41, 42].

In the present study, an I atom coverage of 0.4 was suggested from AES, below the 0.5 needed to form a complete ($\sqrt{2}$ X$2\sqrt{2}$)R45° unit cell (Figure 8b). Figure 9 is an STM

micrograph of the corresponding surface. The arrangement of I atoms appears nearly hexagonal, even though the Au (100) substrate is four-fold symmetric. Also evident in the micrograph are lines of atoms which appear higher than the rest. The periodicity of these streaks are a function of the I atom coverage, with more streaks evident at lower I atom coverages. The I atom coverage is a function of several variables, including time, KI concentration and emersion potential. The crystal used to obtain the micrographs in Figure 9 was oriented with its rows of substrate atoms, the [110] direction, at an angle of 45° with respect to the abscissa of the image, and the $\sqrt{2}$, or [100], direction parallel to the image's abscissa. Taking into account the fact that the streaks propagate at an angle greater than 45° with respect to the rows of I atoms (Figure 9), there are four possible domain orientations, three of which are visible in Figure 10.

Figure 11 is a high contrast copy of the STM micrograph shown in Figure 9, superimposed on a schematic of the Au(100) surface. Figure 11(a) has the substrate positioned so that the I atoms sit in top and four fold sites. If this were the actual site registry, an alternation in the heights of the atoms in the different sites would be expected. Because the I atoms, not involved in streaks, all appear equivalent, the structure shown in Figure 11(b) is suggested, where the substrate is positioned such that all I atoms are in two-fold sites. Two orientations of two-fold sites, are needed to account for the observed micrographs. The unit cell appears to be very close to a ($\sqrt{2}$ X2$\sqrt{2}$)R45°, from examination of Figure 11b. The coverage, determined by AES, was 0.4, not the 0.5 required to form a homogeneous ($\sqrt{2}$ X2$\sqrt{2}$)R45°. This explains the streaks, since the packing density is not sufficient to force the I atoms into the smaller unit-cell. These observations are consistent with the previously mentioned gas phase studies [41, 42].

As suggested above, the streaks appear to be caused by I atoms riding up from the two-fold sites, due to the low packing density, to top sites where they appear as bright steaks. Increased noise frequently accompanies these streaks in the STM images, which is interpreted as

a result of the decreased stability of the I atoms in the top sites. The top site I atoms appear to be moving slightly as the images are recorded. A similar structure has recently been proposed from in-situ STM studies of Au(100) in an I^- solution [38]. Micrographs in that study were equivalent to those obtained in air, shown here.

The image shown in Figure 12 is for the Au(100) surface prepared as described in the experimental section, followed by immersion in the 5 mM KI solution for 5 minutes at -0.1 V. No islands are evident. Large atomically flat terraces were routinely observed after this treatment. Complete removal of the monoatomically high Au islands was achieved even on roughened surfaces, such as that shown in Figure 1, clearly demonstrating the facility of Au electrochemical annealing.

Given atomically flat Au(100) terraces covered with iodine, the next step has been to replace the iodine with Te, if the surface is to be used as a starting point in the formation of CdTe deposits by ECALE. The iodine adlattice can be removed by reduction to I^- at negative potentials, or oxidation to IO_3^- at potentials corresponding to the oxidation of the Au surface itself [43]. However, reductive removal of the iodine layer in a simple electrolyte solution should also result in the reconstruction of the surface, and thus island formation upon switching back to a more positive potential. The alternative method, oxidizing the iodine adlattice off at high potentials, results in the formation of a Au oxide layer which must then be reduced. There is evidence that Au oxidation and reduction contribute to surface roughening [44], as has been observed after oxidation and reduction of Pt surfaces [45] under similar conditions.

There turns out to be a third alternative, to electrodeposit the Te directly onto the I coated substrate. Figure 13b is the voltammetry of the clean six-sided Au(100) crystal in a 0.2 mM TeO_2 solution, pH 1.5. Two UPD features are clearly visible in the negative going scan, one at

0.33V and one at 0.07 V, just prior to a feature corresponding to the bulk deposition of Te. The structural transitions corresponding to these voltammetric features are: formation of an initial Au(100)(2X2)-Te structure at a coverage of 1/4, to a Au(100)(2X$\sqrt{10}$)-Te structure at a coverage of 0.33, to a Au(100)($\sqrt{2}$ X$\sqrt{5}$)-Te structure corresponding to bulk Te, and have been discussed previously [9, 10].

The voltammetry shown in Figure 13c was obtained by using the same electrode, as in 13b, except that an I adlattice was first applied. The initial Te UPD feature (0.33 V in Figure 13b) is completely suppressed, and the second UPD feature appears to be delayed or suppressed as well. Auger spectra of the iodine-precoated electrode emersed at various potentials from the TeO_2 solution, were recorded. Figure 14 shows the Te and I signals for the three faces as a function of the emersion potential. It is clear from Figure 14 that Te does not begin to deposit until about 0.0 V. However, within 100 mV of the start of Te deposition, the iodine is completely displaced; no iodine was detectable on the surface with Auger spectroscopy (Figure 8d). When the Te began to deposit, it formed first on the (100) surface, followed by the (111) and then the (110). A time dependent study has shown the displacement to be a relatively slow process at 0.02 V, taking several minutes, and even longer, for the (110) surface. This displacement of the I atom adlattices can be contrasted with previous studies where Ag and Cu were deposited on iodine adlattices on Au [46] and Pt [47, 48] electrodes. In those studies, the depositing metals combined with the preadsorbed halide layers to form what appeared to be monolayers of the I-VII compounds AgI and CuI, respectively.

The Te structures resulting after iodine displacement, were those corresponding to bulk Te. At potentials where the Te is deposited, bulk Te is stable as well. The bulk Te deposits on Au(100) were well ordered, as can be seen from the LEED pattern shown in Figure 15, corresponding to a ($\sqrt{2}$ X$\sqrt{5}$) unit-cell, also observed after deposition of bulk Te on a clean

Au(100) surface [9]. The STM micrographs corresponding to these bulk deposits show a variety of features. Large flat planes are observed if the charge for deposition is kept low (Figure 16). In our studies a charge equivalent to 1.25 monolayers of Te was found to be more than sufficient to displace the preadsorbed I atom layer. When more bulk Te is deposited, multi-layer Te islands are formed on the surface. Removal of the more extensive bulk Te deposits take correspondingly more time.

The bulk Te structure, responsible for the ($\sqrt{2}$ X$\sqrt{5}$) LEED pattern (Figure 15), is difficult to image with STM. It appears that repeated scanning spreads the Te atoms around, resulting in images such as that shown in Figure 17. A majority of the STM images taken of bulk Te on Au (100) show a structure reminiscent of the (2X$\sqrt{10}$) structure [9]. Some images, however, show the ($\sqrt{2}$ X$\sqrt{5}$) unit-cell. Figure 18 is a proposed atomic arrangement for the first layer of the ($\sqrt{2}$ X$\sqrt{5}$) structure, corresponding to a Te coverage of 2/3.

The first monolayer of CdTe formed on Au(100) deposits epitaxially [49], in a ($\sqrt{2}$ X$\sqrt{2}$)R45°-CdTe structure with 1/2 coverages of Te and Cd. Deposition of this monolayer using the ECALE methodology first involves the formation of a 1/2 coverage Te layer. As deposits of 1.25 monolayers of Te are initially formed, the problem becomes how to remove the excess Te from the surface. In forming the first atomic layer of Te, there are two ways to remove the excess. Because there is no Cd present, the excess Te can be oxidized off the surface, converted to $HTeO_2^+$. Alternatively, the excess Te can be reduced off, converted to Te^{2-}. This second method must be used for subsequent cycles; oxidative removal of the Te would result in oxidation of any Cd present, as well.

In depositing the first atomic layer of Te, the important features appear to be the coverage and lack of island formation. Previous studies have shown that the actual structure of the first Te atomic layer has little effect on the structure of the resulting CdTe layer. However,

if the coverage of Te is too low, the CdTe monolayer will be incomplete [49]; if the coverage of Te is too high, three dimensional nucleation can occur.

Figure 19 is a graph of the Te coverage resulting when a given potential is used to reduce the excess Te from Au(100) in the borate buffered solution. As mentioned previously, Te is initially deposited to the extent that a charge equivalent to 1.25 Te monolayers is passed. The coverages plotted in Figure 19 were determined by integration of the charge required to oxidatively strip the remaining Te. The stripping is performed in the $HTeO_2^+$ solution. A time dependent study, performed at a reduction potential of -1.4 V, indicated that the excess Te was removed within 10 seconds, and that reductions as long as 5 minutes failed to remove more Te (Figure 20). According to Figure 19, a potential of about -1.3V results in a coverage near 0.6. Given that no corrections were made for charging or surface roughness, the actual coverage at -1.3V should approach the ideal 0.5. STM images of the resulting surfaces show large flat terraces, equivalent to the surfaces resulting after the KI treatment (Figure 21). Previous LEED studies [9] have indicated the presence of a $(2X\sqrt{10})$-Te structure under equivalent conditions. Atomic scale STM images confirm the presence of the $(2X\sqrt{10})$ structure on the surfaces (Figure 22). However, this unit cell has previously been ascribed to a 1/3 coverage structure as opposed to the desired 1/2 coverage structure [9, 49].

A graph similar to that shown in Figure 19, but for crystals on which the excess Te was oxidatively removed by poising the crystal at relatively positive potentials for two minutes, is shown in Figure 23. Again, the resulting coverages were obtained by oxidatively stripping the remaining Te, and are uncorrected for charging and surface roughness. Several features are evident in the figure, including two plateaus. The first plateau occurs between about 0.4 and 0.5V. The coverage drops slightly toward higher potentials, but is generally on the low side of 1/2 coverage. Taking into account charging and surface roughness, these coverages should be

even lower. STM images obtained for surfaces corresponding to the plateau are somewhat ambiguous. A number of images recorded under these conditions have indicated the presence of a 1/2 coverage structure that is closely related to a $(2X\sqrt{10})$-Te and a $(\sqrt{2}X\sqrt{2})R45°$-Te (Figure 24). It is clear from previously obtained LEED patterns of the $(2X\sqrt{10})$-Te [9] that the $\sqrt{2}$, or (1/2, 1/2), spots are very prominent, suggesting that the two structures may coexist on the surface. The graph appears to indicate the formation of a 1/2 coverage, $(\sqrt{2}X\sqrt{2})R45°$-Te structure near 0.4V, that converts to a 1/3 coverage $(2X\sqrt{10})$ -Te structure near 0.5V. Figure 25 is a cartoon of these structures and their probable relationship. Similar behavior probably accounts for the coverages and structures observed after reductive removal of the excess Te. The second plateau, between 0.50 and 0.55V clearly corresponds to formation of the 1/4 coverage (2X2) structure (Figure 26) [9, 49].

CONCLUSIONS

A sequence of questions has been addressed concerning the preparation of atomically flat Au single crystal surfaces, specifically, the formation of a half coverage Te adlayer, which is desirable as a first step in the electrodeposition of CdTe by the ECALE methodology. It has been shown that the ORCs, previously used to clean the surface, were contributing to surface roughening, as the reconstruction experienced at low potentials and removed at high potentials formed monoatomically high Au islands on the substrate. It has been shown that treatments in a mM iodide solution result in the electrochemical annealing of the substrate surface, removing the previously formed islands. The procedure results in the formation of large atomically flat terraces, supporting well ordered I adlattices. It has further been shown that Te can be deposited directly on these layers, displacing the I atoms and forming thin films of bulk Te. Finally, it has been shown that the excess, bulk, Te can be removed, either reductively or oxidatively, to form atomic layer of Te with coverages near the ideal 1/2.

ACKNOWLEDGMENTS

This work was supported in part by the Department of the Navy, office of the Chief of Naval Research, under grant # N00014-91-J-1919, and by the National Science Foundation, under grant # DMR-9017431. Their assistance is gratefully acknowledged.

References

1. B.W. Gregory and J.L. Stickney, *J. Electroanal. Chem.* **300,** 543 (1991).

2. B.W. Gregory, D.W. Suggs and J.L. Stickney, *J. Electrochem. Soc.* **138,** 1279 (1991).

3. T. Suntola and J. Antson, U.S. Patent 4,058,430 (1977).

4. S. Bedair, *Atomic Layer Epitaxy,* Elsevier, Amsterdam (1993).

5. T.F. Kuech, P.D. Dapkus and Y. Aoyagi, *Atomic Layer Growth and Processing,* Materials Research Society, Pittsburgh (1991).

6. D.M. Kolb, In *Advances in Electrochemistry and Electrochemical Engineering,* H. Gerischer and C.W. Tobias, Eds., Vol. 11, p. 125. Wiley, New York (1978).

7. K. Jutter and W.J. Lorenz, *Z. Phys. Chem. N.F.* **122,** 163 (1980).

8. R.R. Adzic, In *Advances in Electrochemistry and Electrochemical Engineering,* H. Gerischer and C.W. Tobias, Eds., Vol. 13, p. 159-260. Wiley-Interscience, New York (1984).

9. D.W. Suggs and J.L. Stickney, *J. Phys. Chem.* **95,** 10056 (1991).

10. D.W. Suggs and J.L. Stickney, *Surf. Sci.* **290,** 362 (1993).

11. W.J. McG. Tegart, *The Electrolytic and Chemical Polishing of Metals in Research and Industry,* p. 62. Pergamon Press Ltd., Oxford (1959).

12. I. Villegas and J.L. Stickney, *J. Electrochem. Soc.* **139,** 686 (1992).

13. A. Hamelin, *J. Electroanal. Chem.* **142,** 299 (1982).

14. D.M. Kolb and J. Schneider, *Electrochim. Acta* **31,** 929 (1986).

15. J. Schneider and D.M. Kolb, *Surf. Sci.* **193,** 579 (1988).

16. X. Gao, A. Hamelin and M.J. Weaver, *Phys. Rev. Lett.* **67,** 618 (1991).

17. D.M. Kolb, In *Structure of Electrified Interfaces,* J. Lipkowski and P.N. Ross, Eds., p. 65. VCH Publishers, Inc., New York (1993).

18. X. Gao, G.J. Edens, A. Hamelin and M.J. Weaver, *Surf. Sci.* **296,** 333 (1993).

19. P. Skoluda and D.M. Kolb, *Surf. Sci.* **260,** 229 (1992).

20. X. Gao, A. Hamelin and M.J. Weaver, *Phys. Rev. B.* **46**, 7096 (1992).

21. O.M. Magnussen, J. Hotlos, R.J. Behm, N. Batina and D.M. Kolb, *Surf. Sci.* **296**, 310 (1993).

22. R.C. Jaklevic and L. Elie, *Phys. Rev. Lett.* **60**, 120 (1988).

23. D.J. Trevor, C.E.D. Chidsey and D.N. Loiacono, *Phys. Rev. Lett.* **62**, 929 (1989).

24. D.J. Trevor and C.E.D. Chidsey, *J. Vac. Sci. Technol. B* **9**, 964 (1991).

25. D.R. Peale and B.H. Cooper, *J. Vac. Sci. Technol. A* **10**, 2210 (1992).

26. A. Hamelin, X. Gao and M.J. Weaver, *J. Electroanal. Chem.* **323**, 361 (1992).

27. N. Batina, A.S. Dakkouri and D.M. Kolb, submitted.

28. X. Gao and M.J. Weaver, *J. Phys. Chem.* **97**, 8685 (1993).

29. J.M. Dona and J. Gonzalez-Velasco, *Surf. Sci.* **274**, 205 (1992).

30. F. Sette, T. Hashizume, F. Comin, A.A. MacDowell, and P.H. Citrin, *Phys. Rev. Lett.* **61**, 1384 (1988).

31. B.G. Bravo, S.L. Michelhaugh, M.P. Soriaga, I. Villegas, D.W. Suggs and J.L. Stickney, *J. Phys. Chem.* **95**, 5245 (1991).

32. R.L. McCarley and A.J. Bard, *J. Phys. Chem.* **95**, 9618 (1991).

33. N.J. Tao and S.M. Lindsay, *J. Phys. Chem.* **96**, 5213 (1992).

34. W. Haiss, J.K. Sass, X. Gao and M.J. Weaver, *Surf. Sci.* **274**, L593 (1992).

35. B.M. Ocko, G.M. Watson and J. Wang, *J. Phys. Chem.* **98**, 897 (1994).

36. X. Gao, G.J. Edens and M.J. Weaver, *J. Phys. Chem.* submitted.

37. X. Gao and M.J. Weaver, *Ber. Bunsenges. Phys. Chem.* **97**, 507 (1993).

38. X. Gao, G.J. Edens, F.-C. Liu and M.J. Weaver, *J. Phys. Chem.* submitted.

39. J.L. Stickney, C.B. Ehlers, and B.W. Gregory, *Langmuir* **4**, 1368 (1988).

40. L. Pauling, *The Nature of the Chemical Bond,* 3rd edn, p. 260. Cornell University Press, Ithaca (1960).

41. A. Neumann, K. Christmann, and T. Solomun, *Surf. Sci.* **287/288**, 593 (1993).

42. G.A. Garwood and A.T. Hubbard, *Surf. Sci.* **92**, 617 (1980).

43. J.F. Rodriguez and M.P. Soriaga, *J. Electrochem. Soc.* **135**, 616 (1988).

44. X. Gao and M.J. Weaver, *J. Electroanal. Chem.* submitted.

45. F.T. Wagner and P.N. Ross, *Surf. Sci.* **160**, 305 (1985).

46. S. Sugita, T. Abe and K. Itaya, *J. Phys. Chem.* **97**, 8780 (1993).

47. J.L. Stickney, S.D. Rosasco, D.Song, M.P. Soriaga and A.T. Hubbard, *Surf. Sci.* **130**, 326 (1983).

48. J.L. Stickney, S.D. Rosasco and A.T. Hubbard, *J. Electrochem. Soc.* **131**, 260 (1983).

49. D.W. Suggs and J.L. Stickney, *Surf. Sci.* **290**, 375 (1993).

50. N.N. Greenwood and A. Earnshaw, *Chemistry of the Elements*, Pergamon Press, Oxford (1984).

Figure Captions

Figure 1
STM micrograph showing monoatomically high Au islands on a clean Au(100) surface.
V_b = 109.9 mV, i_t = 1.0 nA, Z range = 5.0 nm.

Figure 2
STM micrograph showing both the reconstructed and unreconstructed Au(100).
V_b = 29.5 mV, i_t = 37.4 nA, Z range = 0.4 nm.

Figure 3
STM micrograph showing island formation on a clean Au(100) surface.
V_b = 28.2 mV, i_t = 6.1 nA, Z range = 1.3 nm.

Figure 4
LEED pattern from a Au(110) surface exposed to an iodide solution at open circuit potential (-0.16 V). 66.4 eV. Au(110)(3X2)-I

Figure 5
STM micrograph of a Au(110) surface exposed to an iodide solution at open circuit potential (-0. 35 V). V_b = 22.1 mV, i_t = 5.6 nA, Z range = 0.3 nm.

Figure 6
Structure proposed to account for Au(110)(3X2)-I. The van der Waals radius for I (0.215 nm) [40] and the metal radius (12-coordinate) for Au (1.44 A)[50] were used.

Figure 7
LEED pattern from a Au(100) surface exposed to an iodide solution at open circuit potential (-0.16 V). 40.7 eV.

Figure 8
Auger spectra taken of a Au(100) surface after:
a) ion bombardment cleaning and annealing
b) I treatment at open circuit potential (-0.16 V)
c) initial deposition of Te on I-treated electrode (0.00 V)
d) bulk Te (-0.20 V)
e) reductive dissolution of bulk Te (-1.30 V)

Figure 9
STM micrograph of a Au(100) surface exposed to an iodide solution (-0.10 V).
V_b = 18.9 mV, i_t = 7.5 nA, Z range = 0.3 nm.

Figure 10
STM micrograph of a Au(100) surface exposed to an iodide solution (0.00 V).
V_b = 12.0 mV, i_t = 5.2 nA, Z range = 2.0 nm.

Figure 11
Proposed structure for I on Au(100)
a) Four fold and top sites
b) Two fold sites

Figure 12
STM micrograph of an iodide treated Au(100) surface, showing large terraces, without islands.
V_b = 22.1 mV, i_t = 9.0 nA, Z range = 1.0 nm.

Figure 13
Au (100) Voltammetry
a) Clean Au(100) in 20 mM H_2SO_4, scan rate 5 mV/sec.
b) Te deposition on clean Au(100) in 0.2 mM TeO_2, pH=1.5, scan rate 2 mV/sec.
c) Te deposition on I-treated Au(100) in 0.2 mM TeO_2, pH=1.5, scan rate 2 mV/sec.
d) Stripping of Te UPD in 0.2 mM TeO_2, after reductive removal of bulk at -1.30 V for two minutes, pH=1.5, scan rate 2 mV/sec.
e) Stripping of Te UPD in 0.2 mM TeO_2, after oxidative removal of bulk at 0.40V for two minutes, pH=1.5, scan rate 2 mV/sec.

Figure 14
AES intensities for Te and I as a function of potential for the three low index planes.
a) Au(100)
b) Au(111)
c) Au(110)

Figure 15
LEED pattern observed after deposition of bulk Te on Au(100). 39.1 eV.
Au(100)($\sqrt{2}$ X$\sqrt{5}$)-Te

Figure 16
STM micrograph of bulk Te on Au(100) formed by displacing I with Te.
V_b = 25.2 mV, i_t = 5.1 nA, Z range = 0.4 nm.

Figure 17
STM micrograph of bulk Te on Au(100) formed by displacing I with Te. The structure corresponds to a Au(100)(2X$\sqrt{10}$)-Te. V_b = 13.9 mV, i_t = 5.0 nA, Z range = 0.5 nm.

Figure 18
Drawing depicting the Au(100)($\sqrt{5}$ X$\sqrt{2}$)-Te structure. The atomic radius (12-coordinate) for Te (1.60 A) [50] and the metal radius (12-coordinate) for Au (1.44 A)[50] were used.

Figure 19
The Te coverage remaining after reductive dissolution of excess Te is plotted as a function of the reduction potential used, for the Au(100) surface.

Figure 20
The Te coverage remaining after reductive dissolution, as a fuction of time, at -1.4 V on the Au(100) surface.

Figure 21
STM micrograph after reduction of bulk Te at -1.4 V.
V_b = 27.2 mV, i_t = 10.8 nA, Z range = 1.0 nm.

Figure 22
STM micrograph of Au(100)(2X$\sqrt{10}$)-Te obtained after reduction of bulk Te at -1.4 V.
V_b = 27.2 mV, i_t = 10.8 nA, Z range = 0.4 nm.

Figure 23
The Te coverage remaining after oxidative dissolution of excess Te is plotted as a function of the oxidation potential used, for the Au(100) surface.

Figure 24
STM micrograph of Au(100)($\sqrt{2}$ X$\sqrt{2}$)R45°-Te, obtained after oxidative dissolution of bulk Te at 0.38 V. V_b = 20.4 mV, i_t = 2.4 nA, Z range = 0.3 nm.

Figure 25
Drawing depicting the Au(100)(2X$\sqrt{10}$)R45°-Te structure and the Au(100)($\sqrt{2}$ X$\sqrt{2}$)-Te structure. The atomic radius (12-coordinate) for Te (1.60 A) [50] and the metal radius (12-coordinate) for Au (1.44 A)[50] were used.

Figure 26
STM micrograph of Au(100)(2X2)-Te. V_b = 36.4 mV, i_t = 5.3 nA, Z range = 0.3 nm.

Figure 1 - L.B. Goetting, B.M. Huang, T.E. Lister & J.L. Stickney

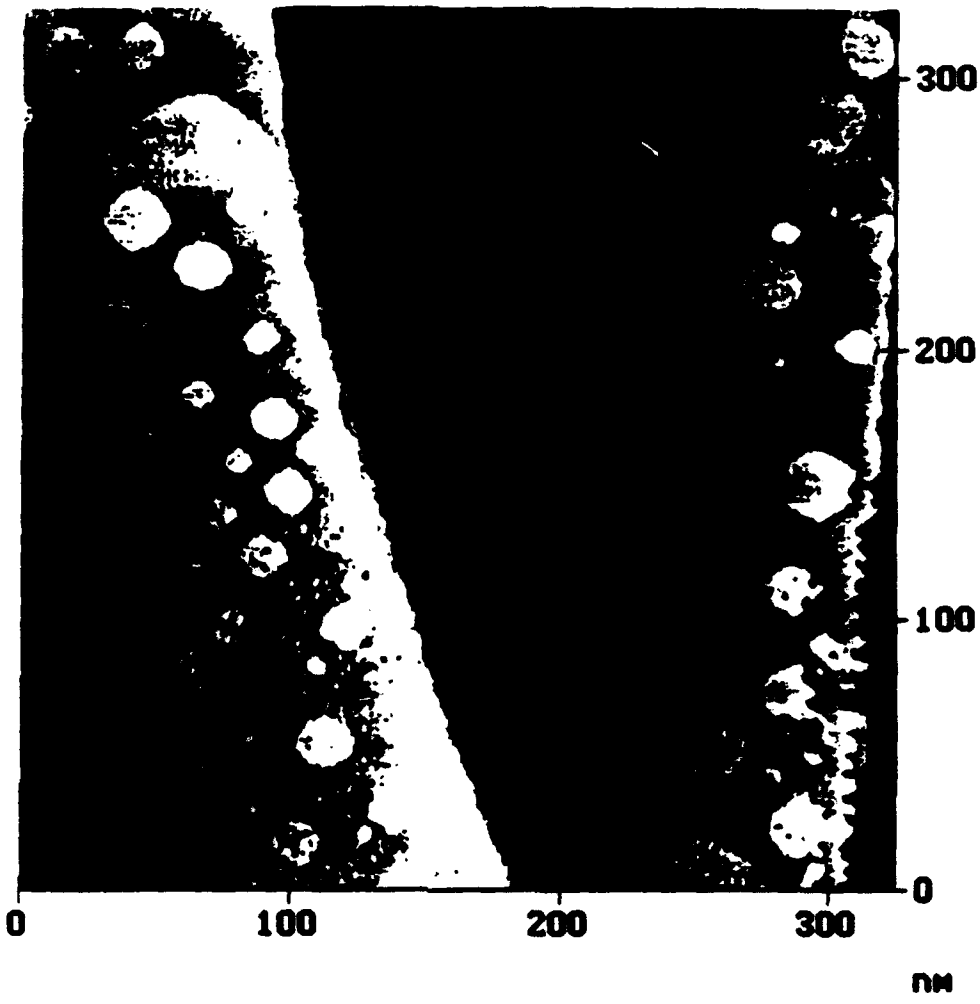

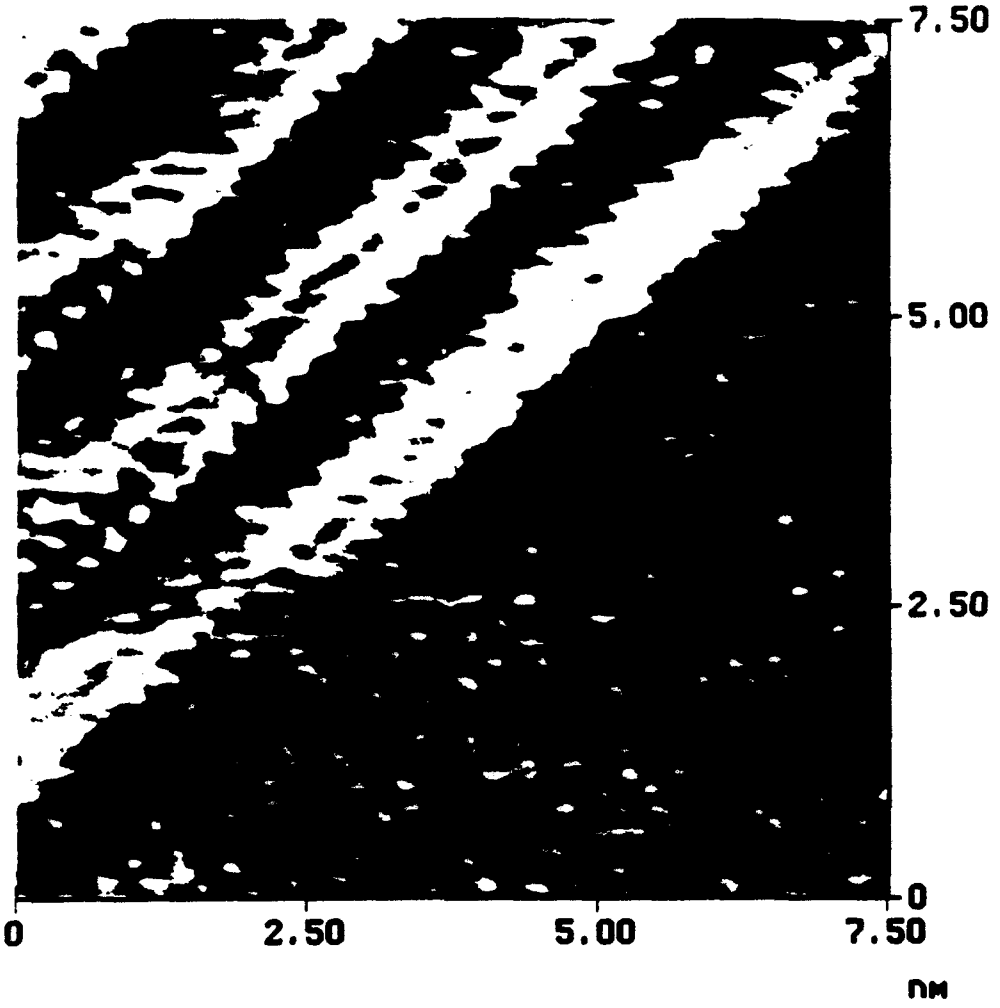
7.50
5.00
2.50
0
0
2.50
5.00
7.50
nm

Figure [illegible]

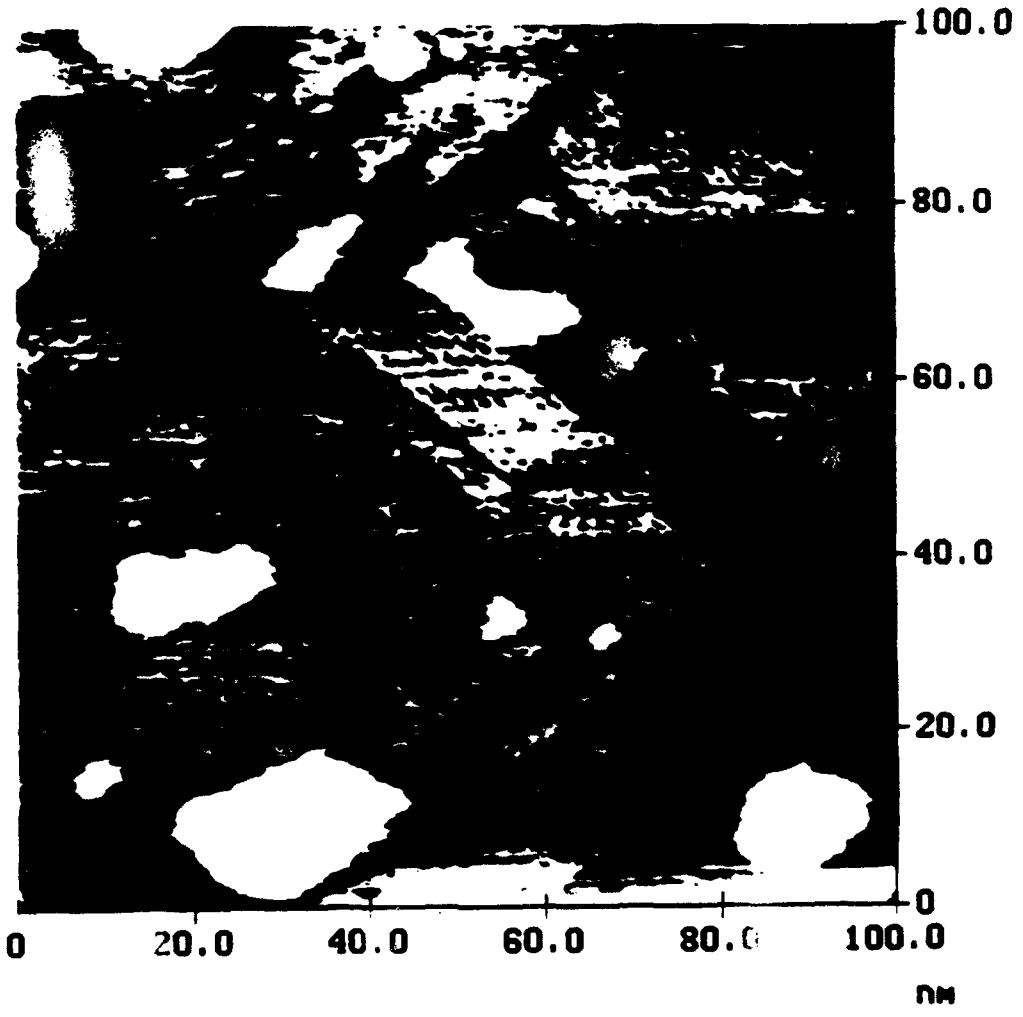

Figure 4 - L.B. Goetting, B.M. Huang, T.E. Lister & J.L. Stickney

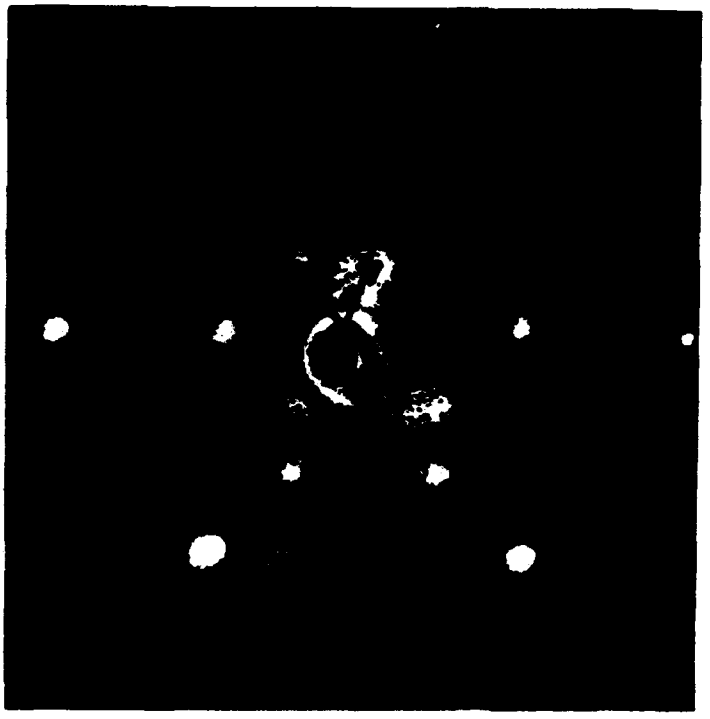

Figure 5 - L.B. Goetting, B.M. Huang, T.E. Lister & J.L. Stickney

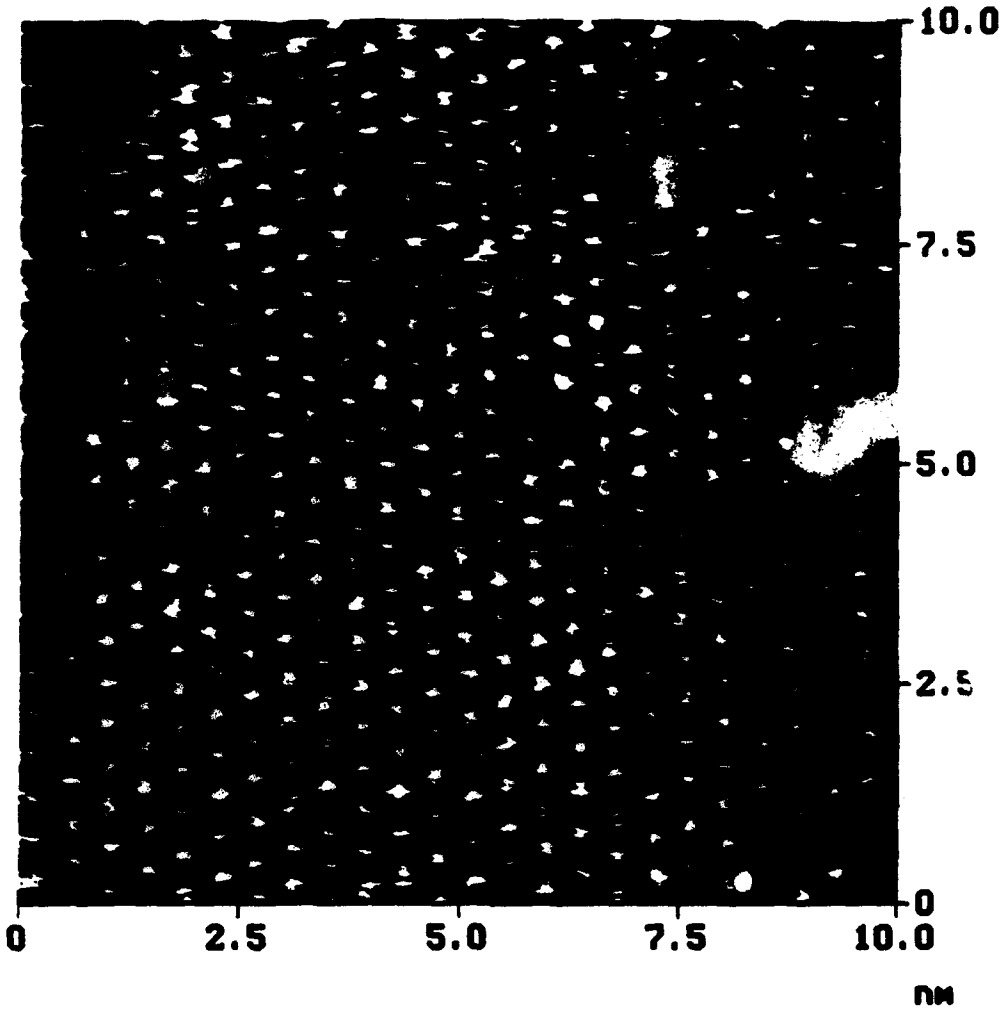

Figure 6 - L.B. Goetting, B.M. Huang, T.E. Lister, & J.L. Stickney

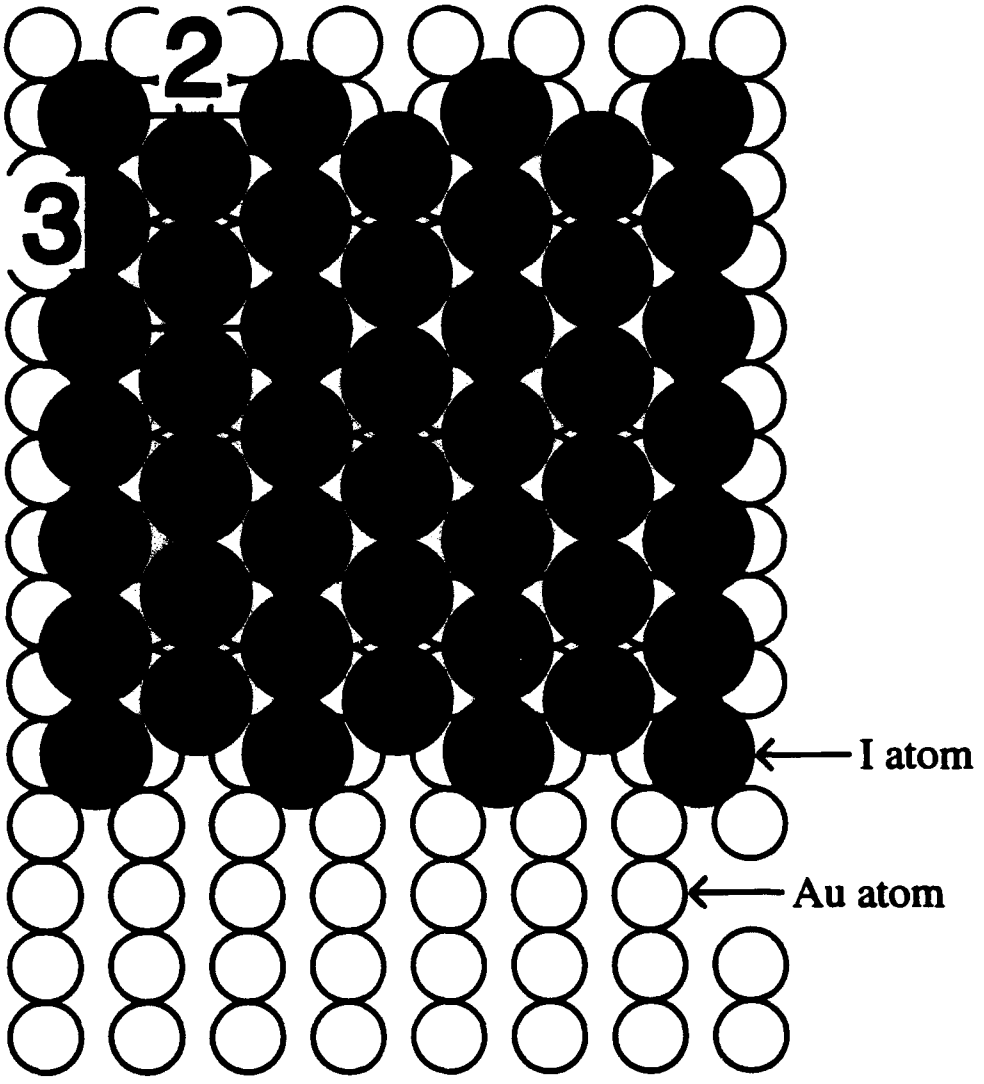

Figure 7 - L.B. Goetting, B.M. Huang, T.E. Lister, & J.L. Stickney

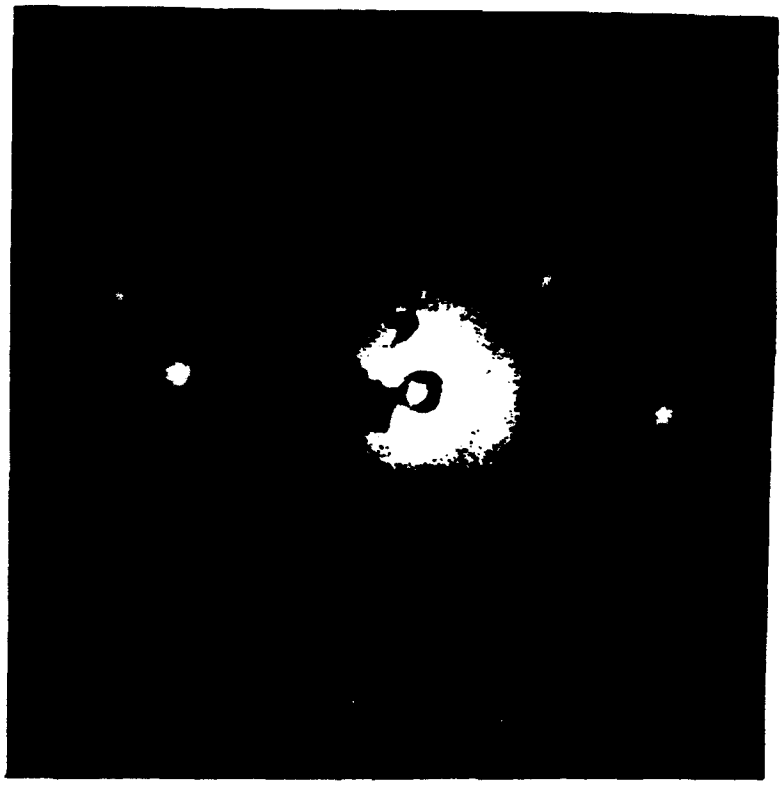

Figure 8 - L.B. Goetting, B.M. Huang, T.E. Lister, & J.L. Stickney

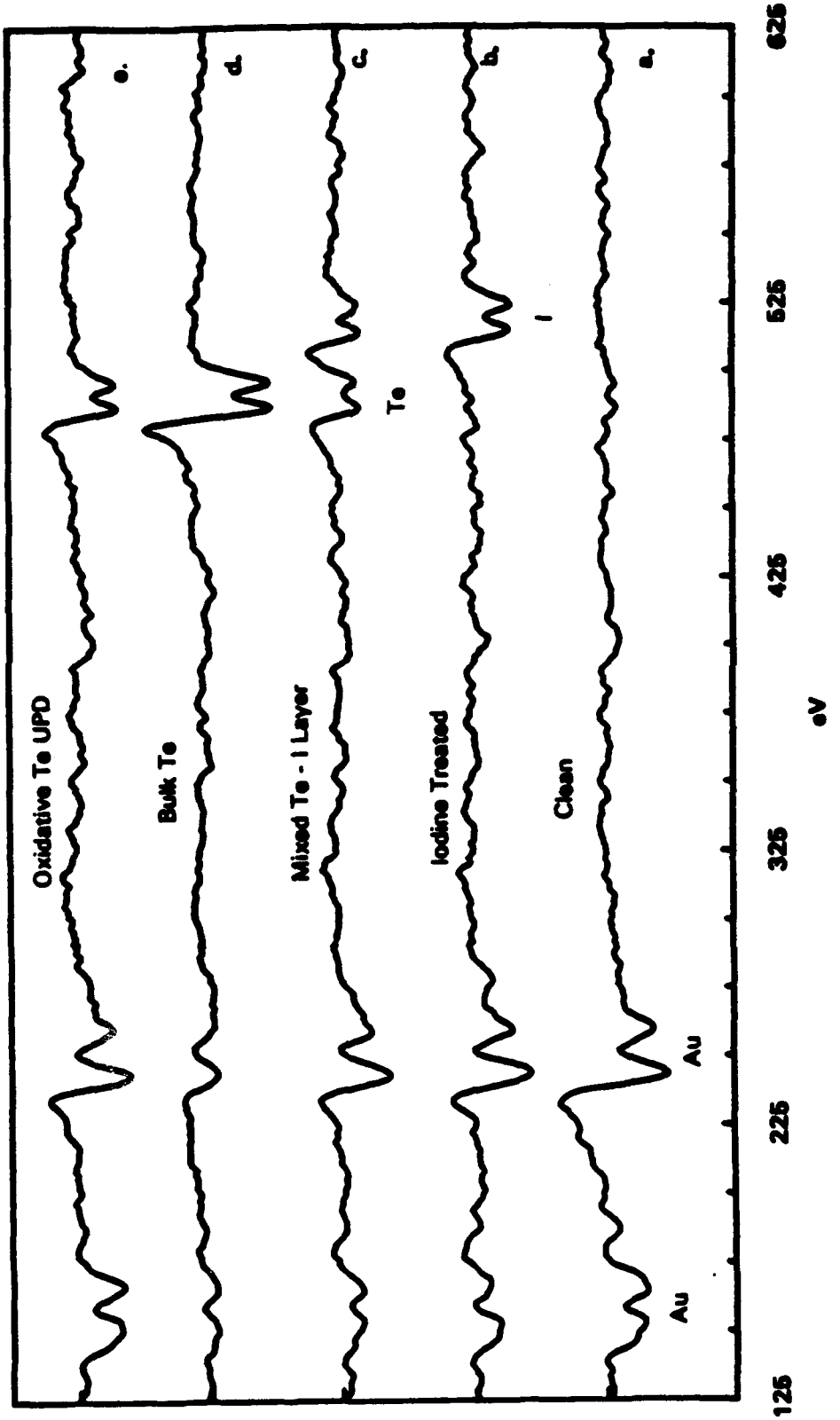

Figure 9 - L.B. Goetting, B.M. Huang, T.E. Lister & J.L. Stickney

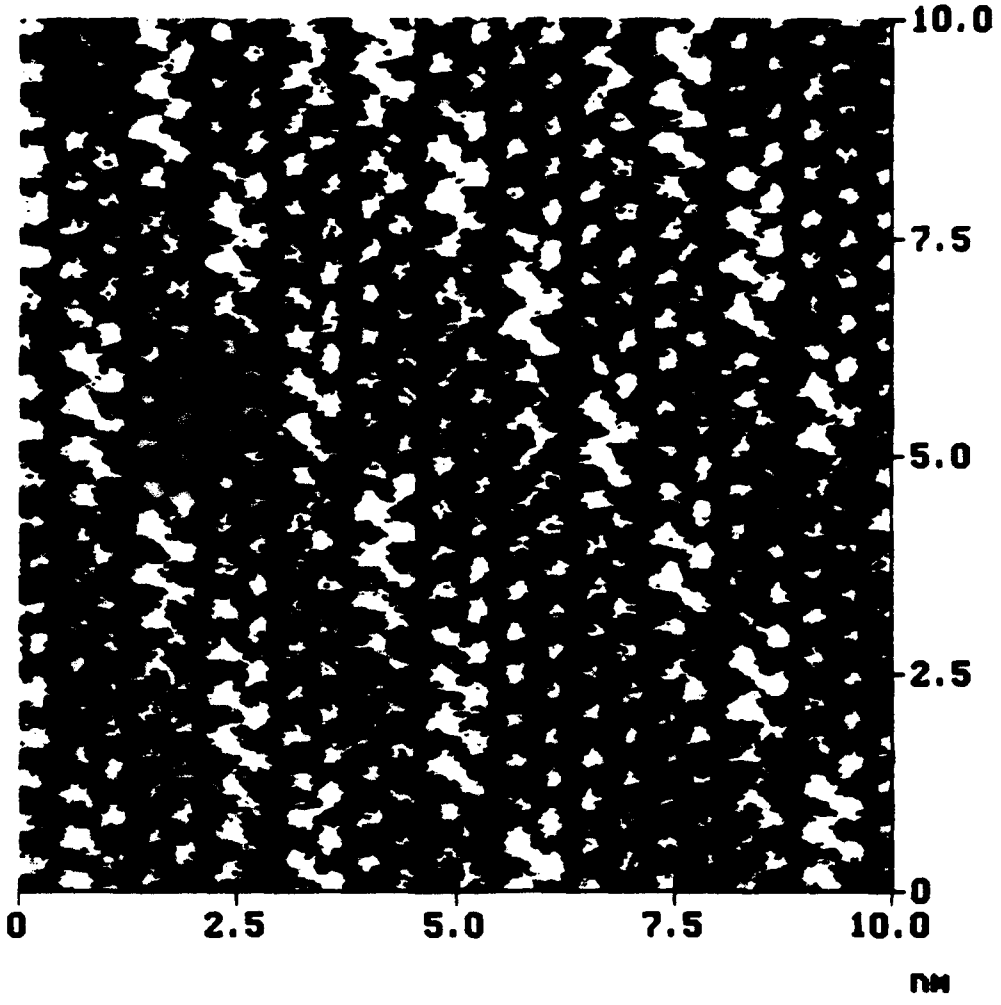

Figure 11 - 1 Goetting, B.M. Huang, T.E. Lister & J.L. Stickney

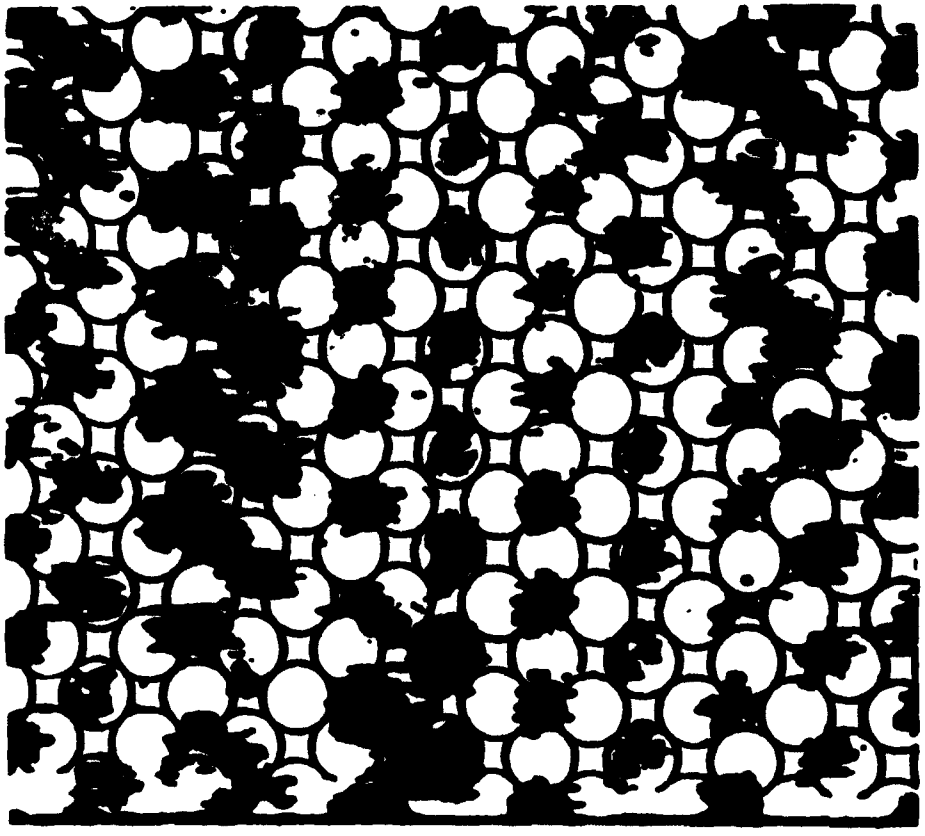

a) Four Fold and Top Sites

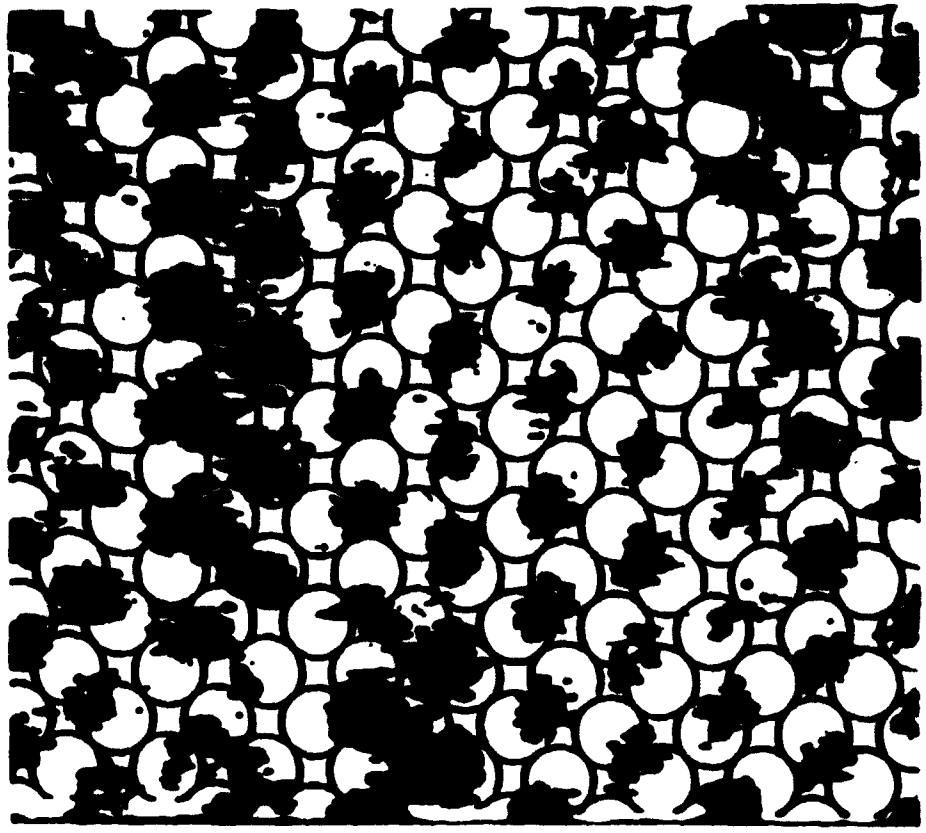

b) Two Fold Sites

Figure 10 - L.B. Goetting, B.M. Huang, T.E. Lister & J.L. Stickney

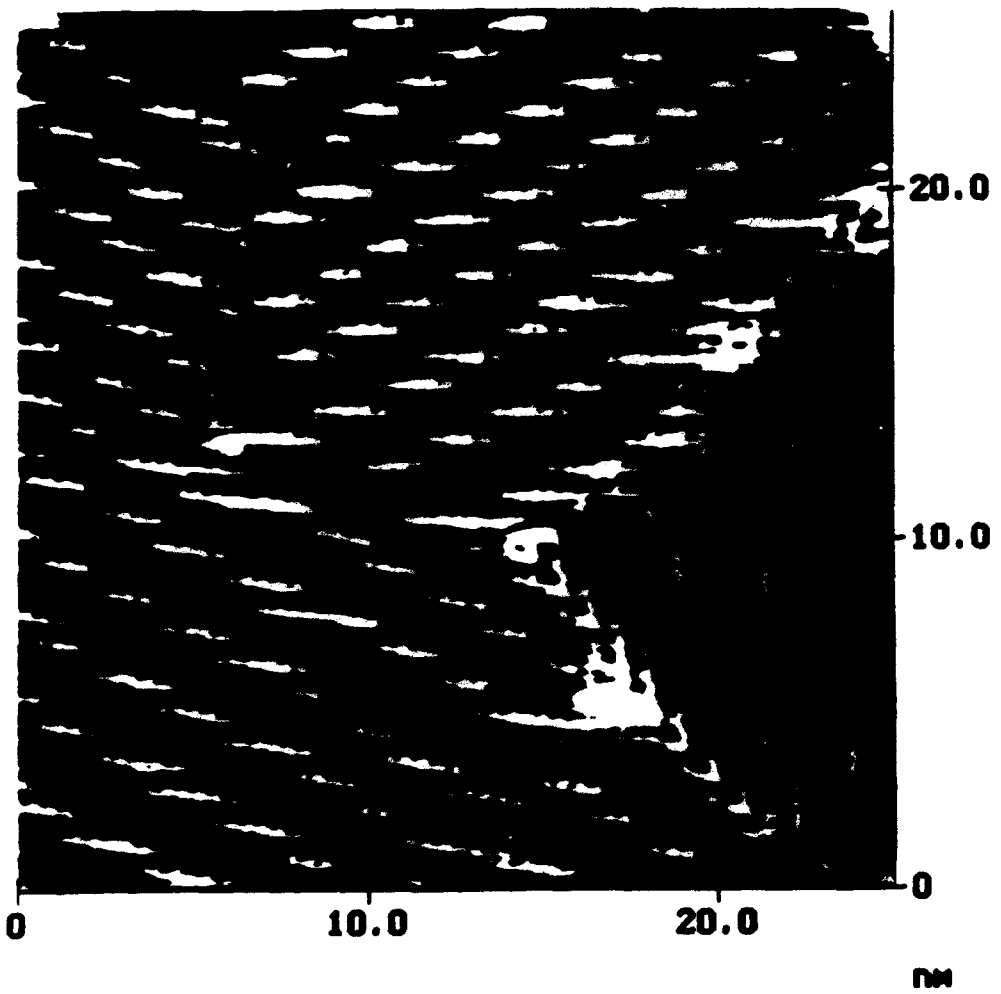

Figure 1_ - L.B. Goetting, B.M. Huang, ...

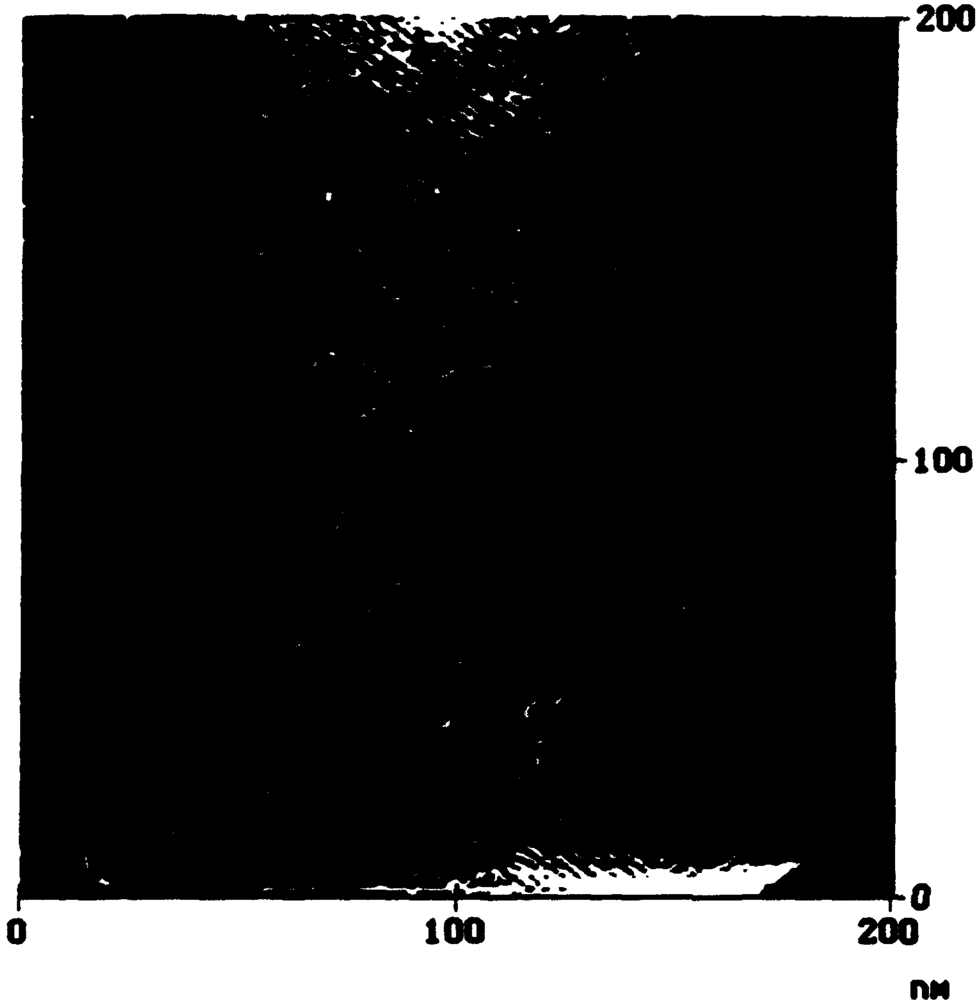

Figure 13 - L.B. Goetting, ..M. Huang, T.E. Lister & J.L. Stick..y

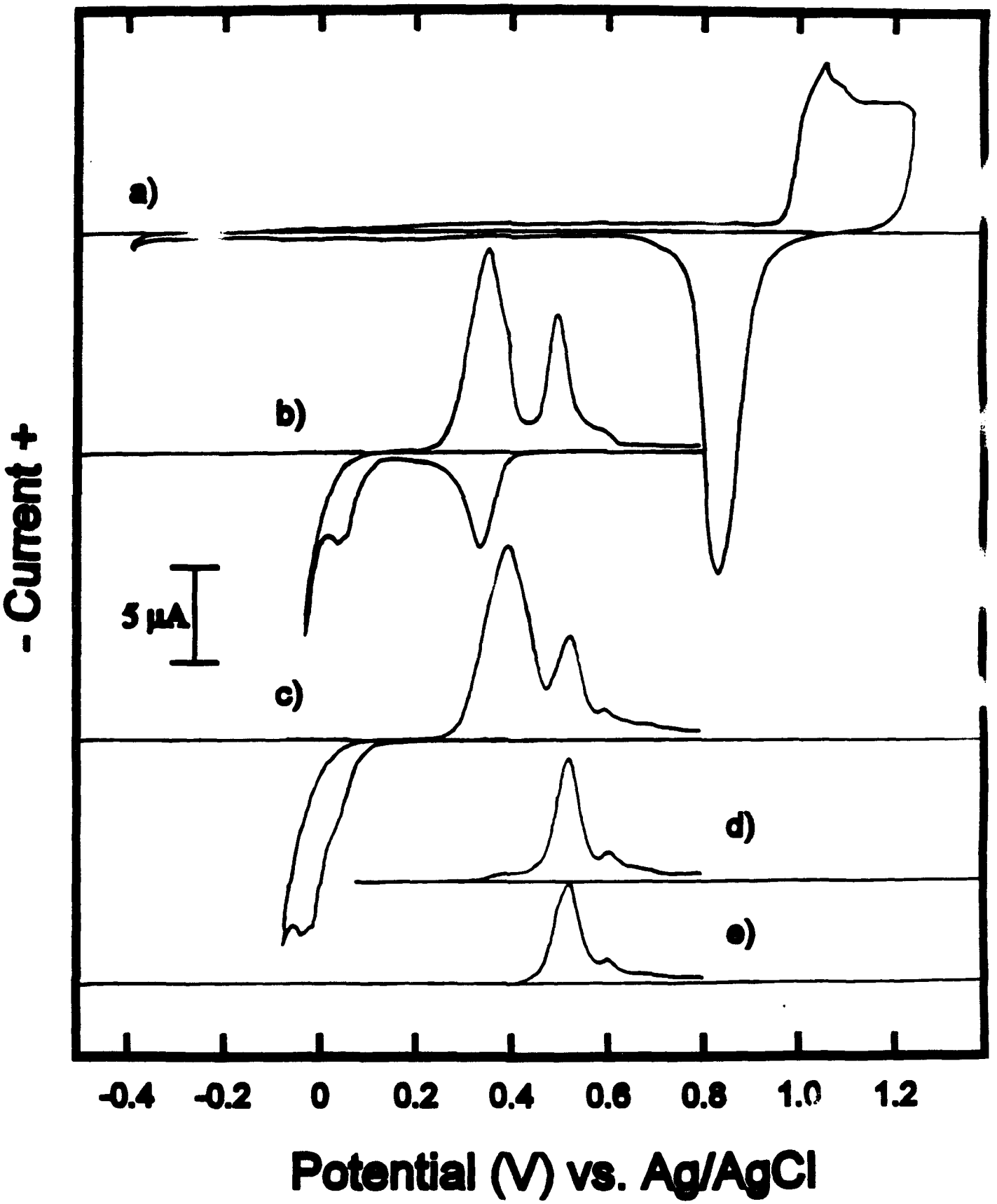

Figure 14 - L.B. Goetting, B.M. Huang, T.E. Lister, & J.L. Stickney

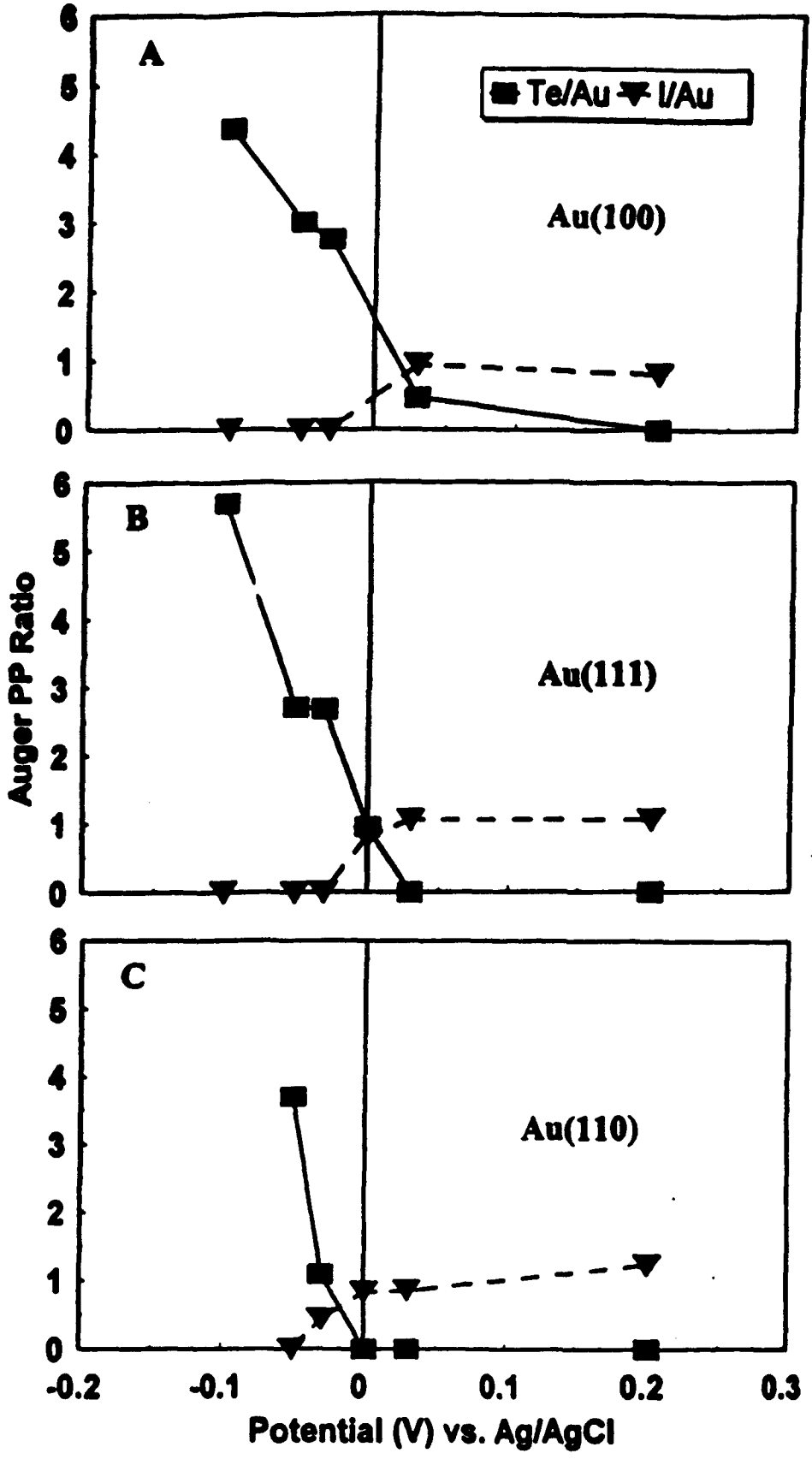

Figure 15 - L.B. Goetting, B.M. Huang, T.E. Lister & J.L. Stickney

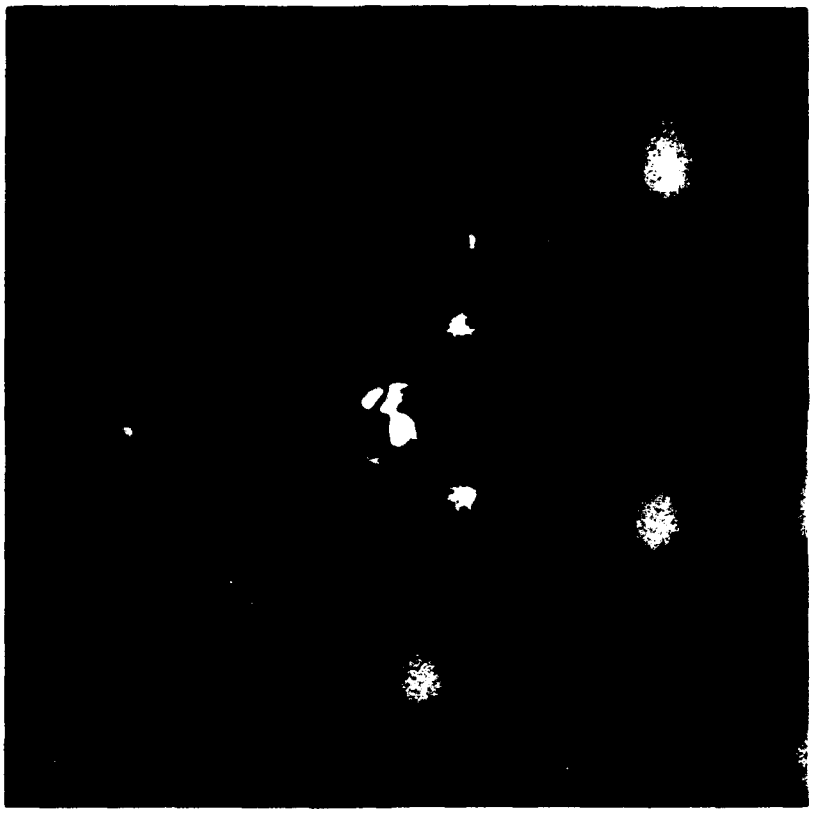

Figure 16 - L.B. Goetting, B.M. Huang, T.E. Lister & J.L. Stickney

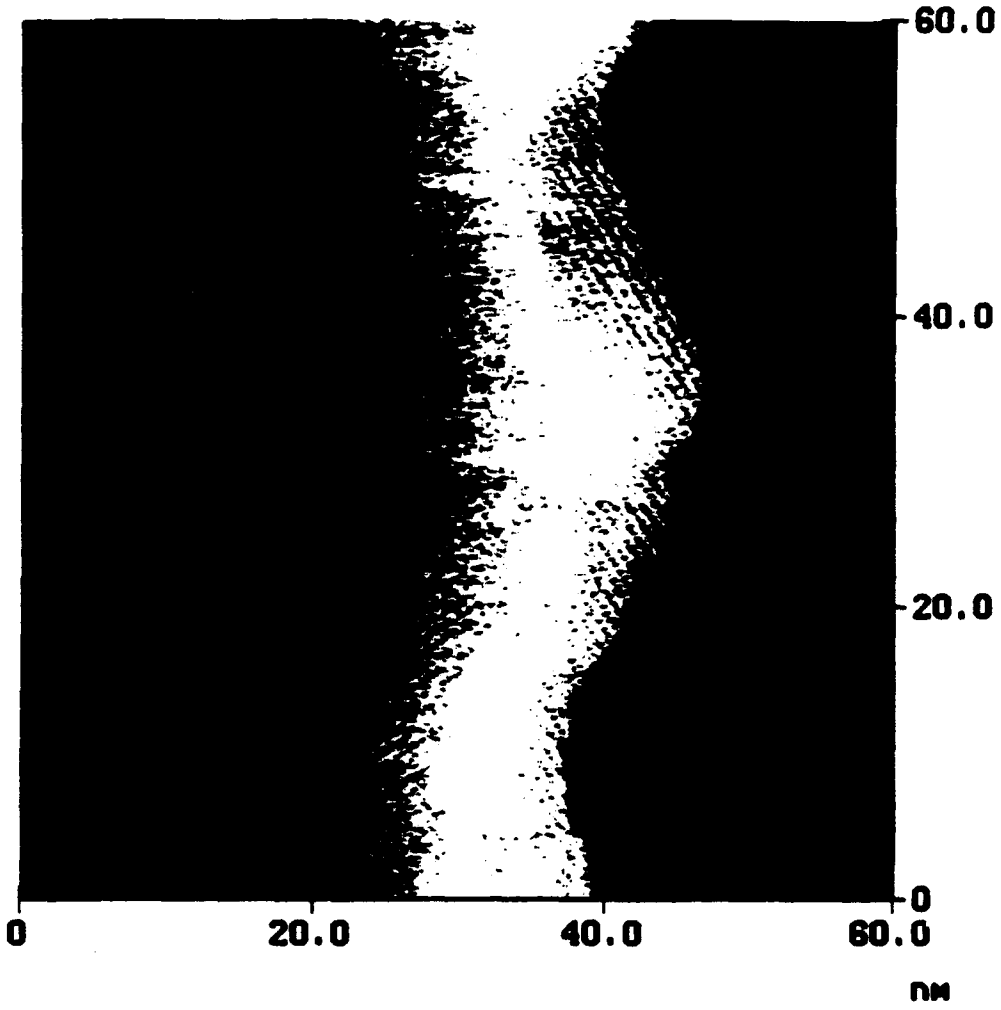

Figure 1 - L.B. Goetting, B.M. Huang, T.E. Lister & J.L. Stickney

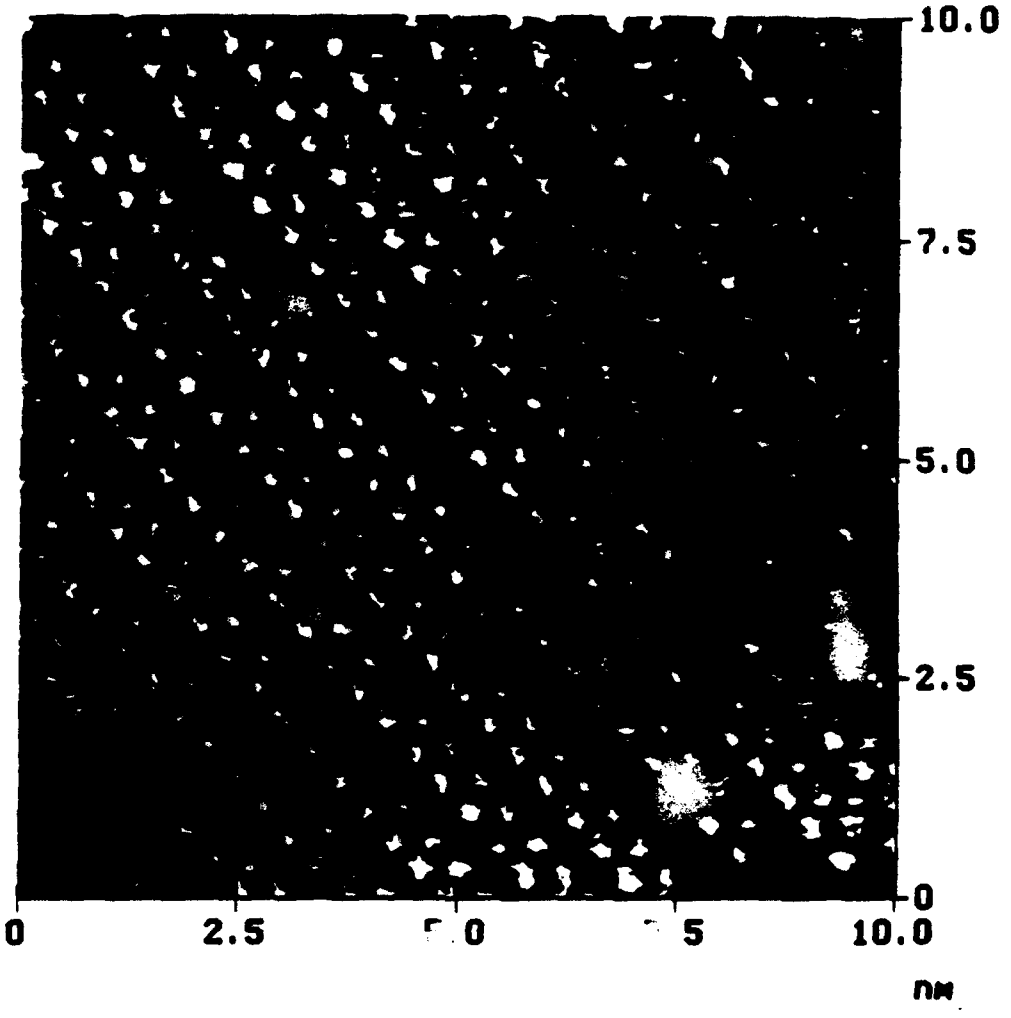

Figure 19 - L.B. Goetting, B.M. Huang, T.E. Lister & J.L. Stickney

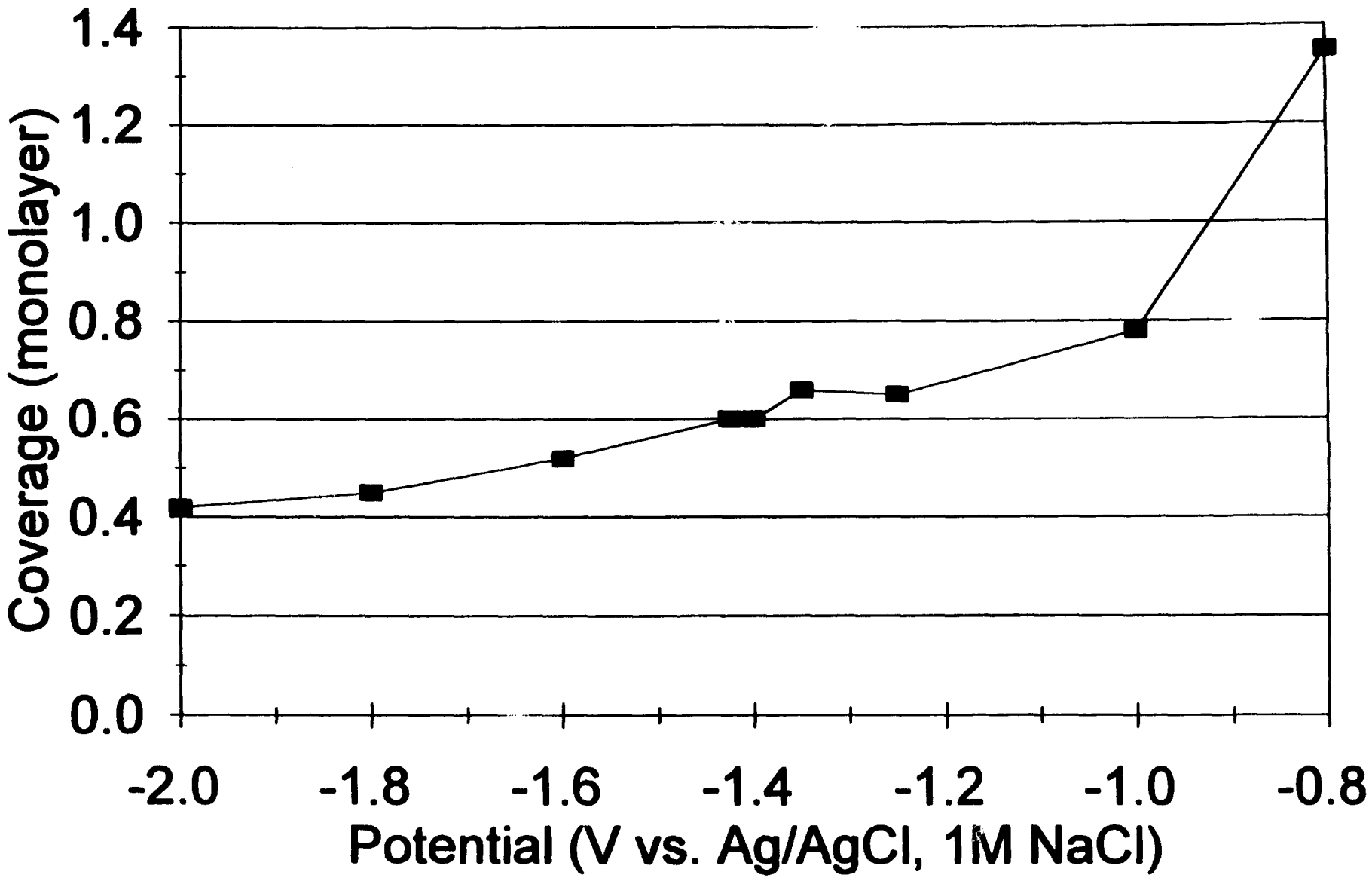

Figure 18 - L.B. Goetting, B.M. Huang, T.E. Lister, & J.L. Stickney

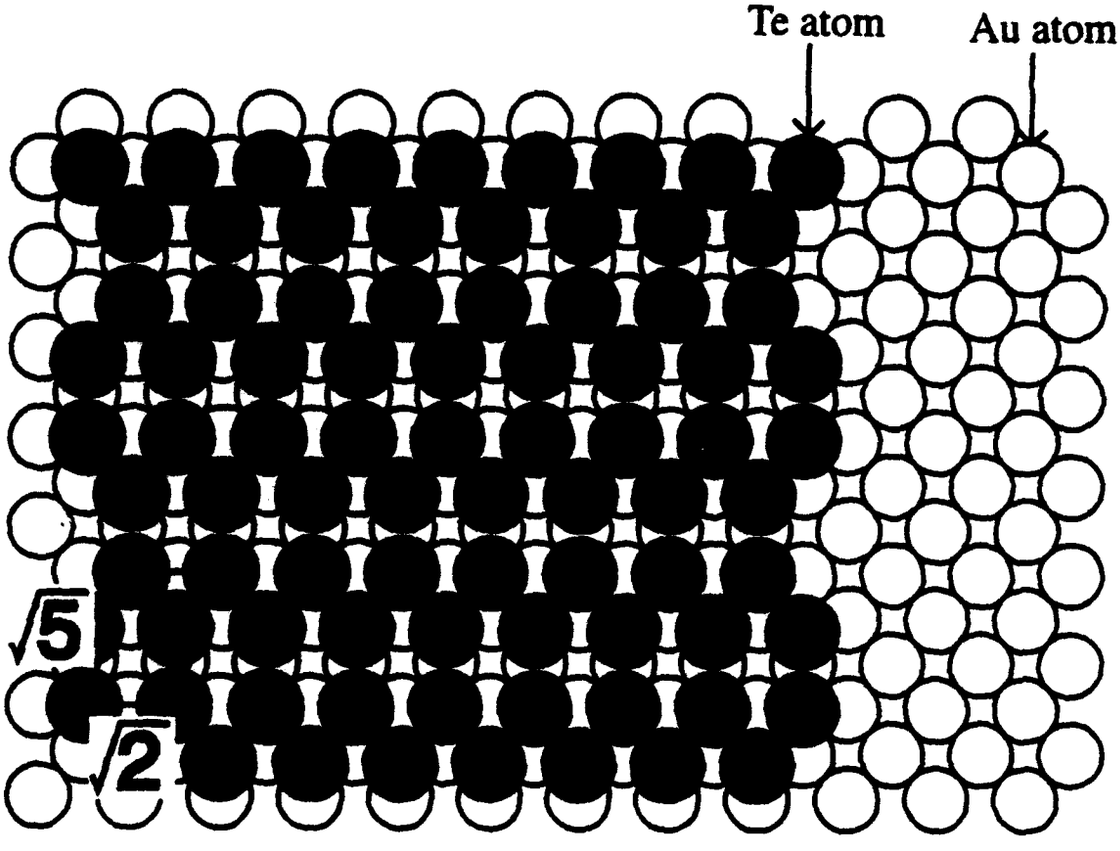

Figure 21 - L.B. Goetting, B.M. Huang, T.E. Lister & J.L. Stickney

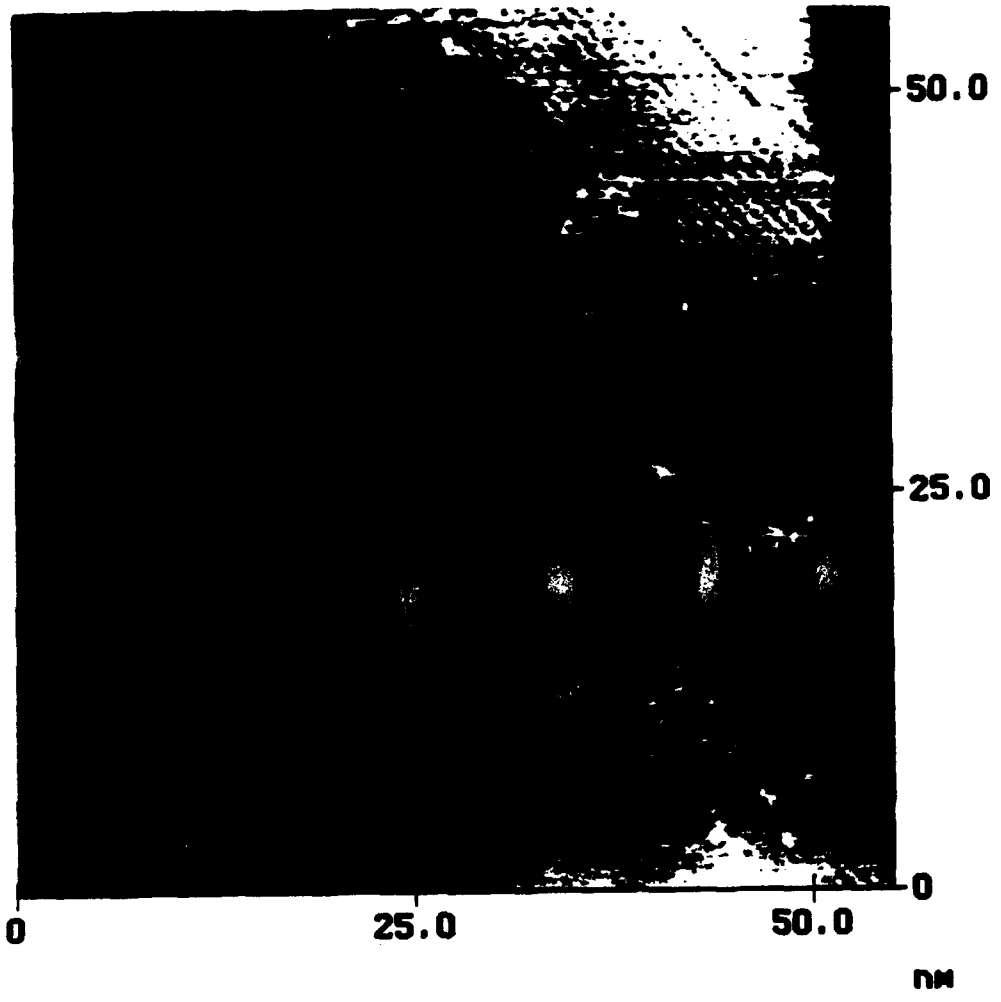

Figure 20 - L.B. Goetting, B.M. Huang, T.E. Lister & J.L. Stickney

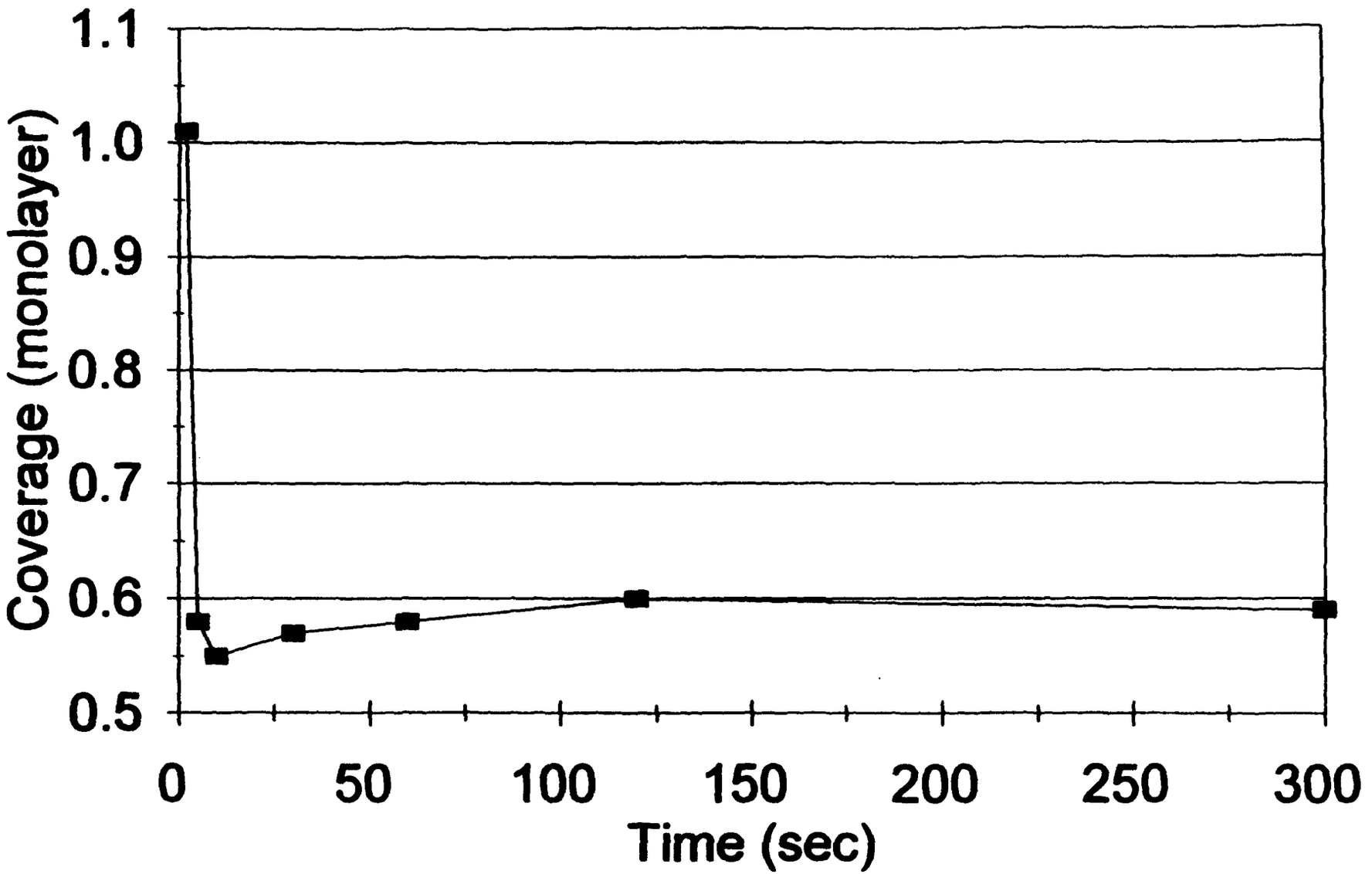

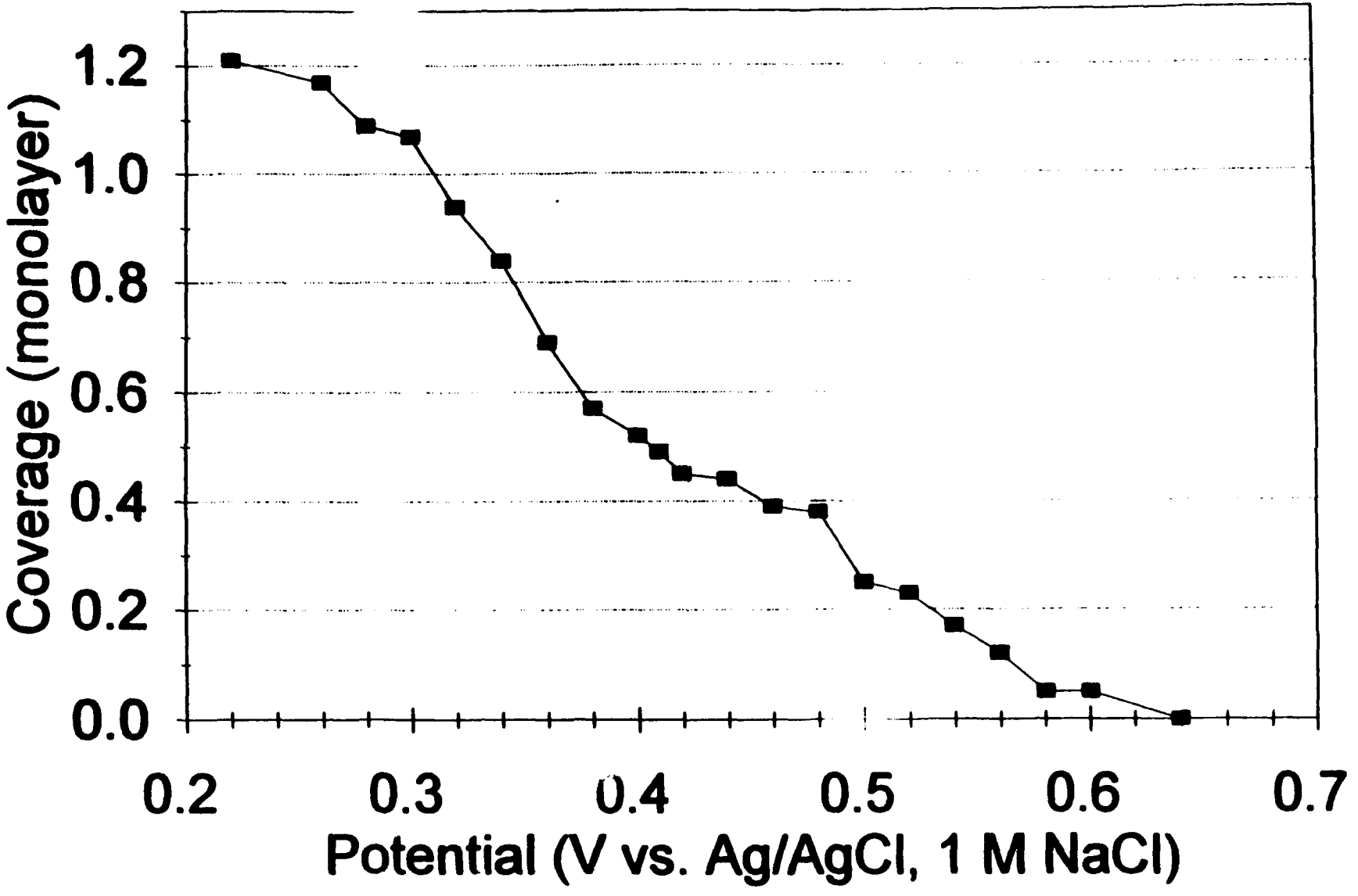
Coverage (monolayer)
1.2
1.0
0.8
0.6
0.4
0.2
0.0
0.2
0.3
0.4
0.5
0.6
0.7
Potential (V vs. Ag/AgCl, 1 M NaCl)

Figure 22 - L.B. Goetting, B.M. Huang, T.E. Lister & J.L. Stickney

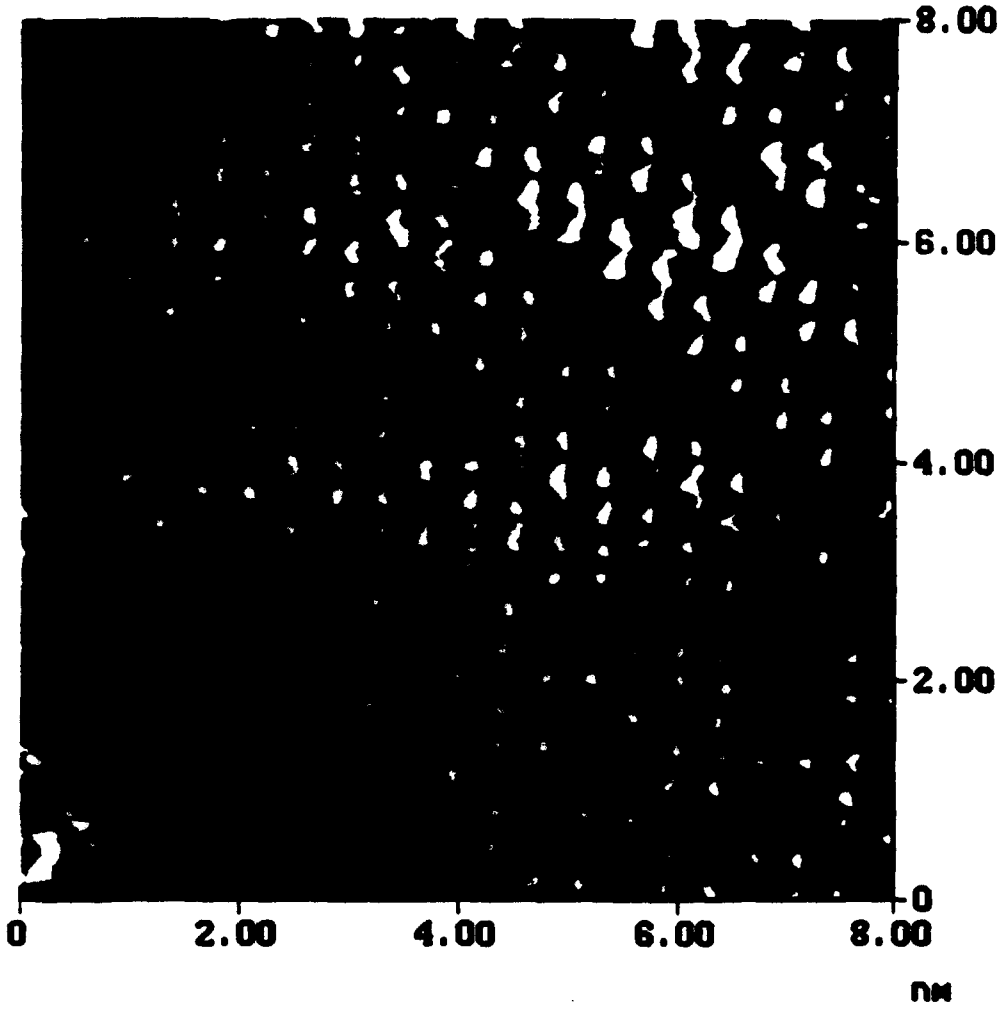

Figure 24 - L.B. Goetting, B.M. Huang, T.E. Lister & J.L. Stickney

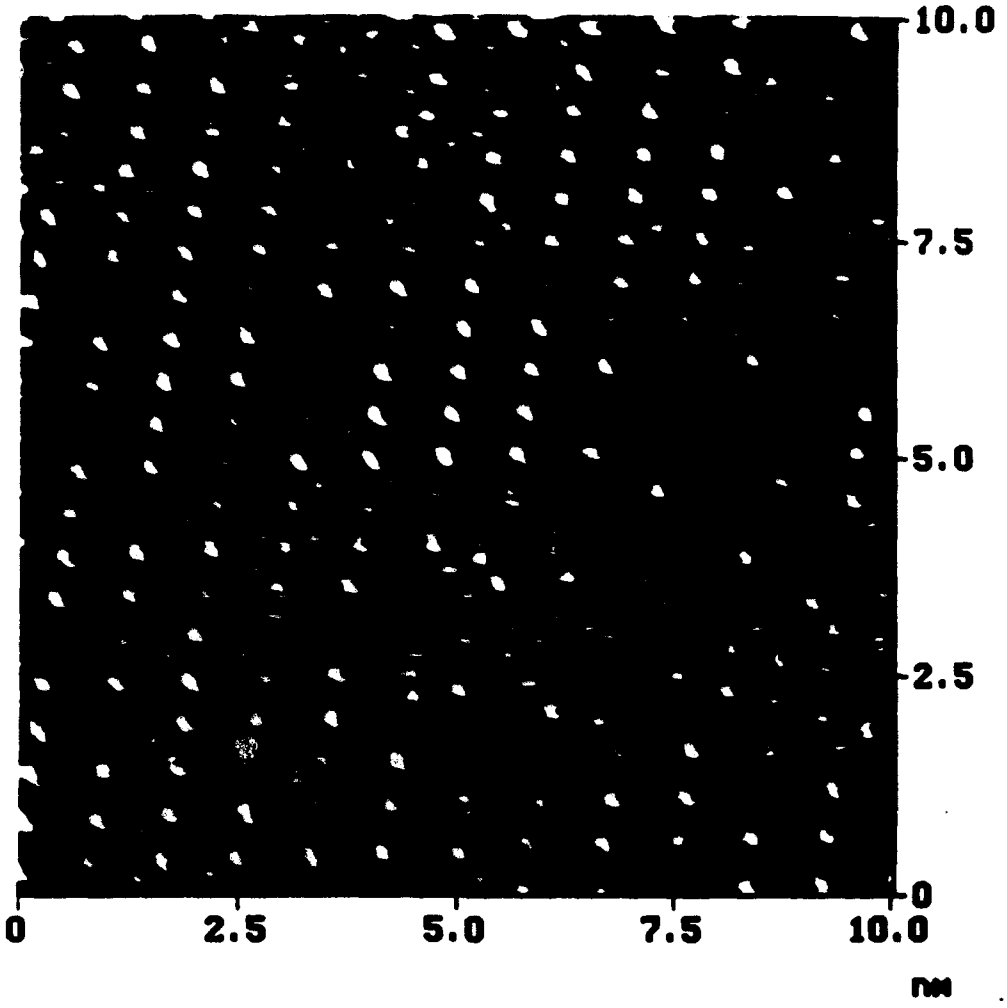

Figure 25 - L.B. Goetting, B . Huang, T.E. Lister, & J.L. Stickney

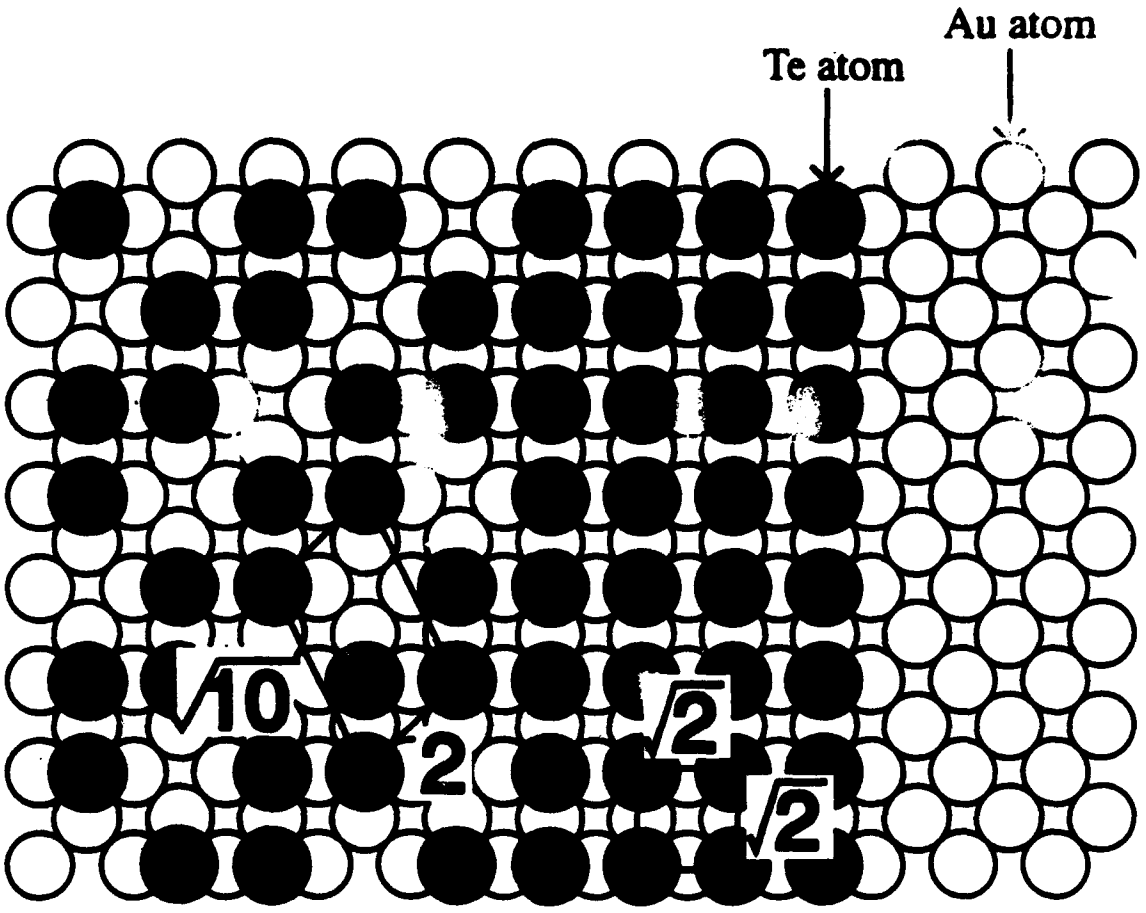

Figure 26 - L.B. Goetting, B.M. Huang, T.E. Lister & J.L. Stickney